Title
AN APPLICATION OF FRACTURE MECHANICS TO GLASSY PLASTICS

Authors
Key, P.L.
Katz, Y.
Parker, E.R.

Publication Date
1968-02-01

UCRL-17911

University of California

Ernest O. Lawrence Radiation Laboratory

AN APPLICATION OF FRACTURE MECHANICS TO GLASSY PLASTICS

P. L. Key, Y. Katz and E. R. Parker

February 1968

DISCLAIMER

UCRL-17911
UC-25 Metals,
Ceramics and Materials
TID-4500 (51st Ed.)

UNIVERSITY OF CALIFORNIA

Lawrence Radiation Laboratory
Berkeley, California

AEC Contract No. W-7405-eng-48

AN APPLICATION OF FRACTURE MECHANICS TO GLASSY PLASTICS

P. L. Key, Y. Katz and E. R. Parker

February 1968

AN APPLICATION OF FRACTURE MECHANICS TO GLASSY PLASTICS

P. L. Key, Y. Katz and E. R. Parker

Inorganic Materials Research Division, Lawrence Radiation Laboratory,
Department of Mineral Technology, College of Engineering,
University of California, Berkeley, California

ABSTRACT

The use of linear elastic fracture mechanics to evaluate the effects of cracks in glassy plastics is reviewed. Plane strain fracture toughness values are obtained for polystyrene, polycarbonate, acrylic and a vinyl chloride-vinyl acetate copolymer. A strong dependence of fracture toughness on temperature and on strain rate at high strain rates is observed for polycarbonate and acrylic tested in the range of 123°K to 348°K and 10^{-3} to 5 cm/min. Adequate agreement is observed among fracture toughness values obtained using single edge notch specimens, notched round specimens, and center notch specimens thus confirming currently recommended specimen designs for fracture toughness determination.

I. INTRODUCTION

The object of fracture mechanics is to provide the designer with a procedure and necessary material properties for considering the effects of flaws on a structure replacing other techniques, such as impact testing and notch tensile tests which do not lend themselves readily to design. The basic ideas of fracture mechanics were developed by Irwin[1] during a period in which fracture work was stimulated by the liberty ship failures of World War II. These ideas have been further developed and widely exploited under the stimulus of the demanding requirements of the aerospace and nuclear industries. Several reviews[2,3] and books,[4,5] devoted solely to fracture or fracture mechanics are now available.

Although applications of fracture mechanics to metals have been numerous, similar applications to glassy plastics have been infrequent. With the exception of the work of van der Boogaart and Turner,[6] the investigation of fracture of plastics is generally done either by impact testing or by a classical application of Griffith's ideas to a cleavage situation such as the work of Berry.[7] The present work had several objectives. First, the application of fracture mechanics to glassy plastics was illustrated by determining the plane strain fracture toughness of several commercial plastics. The term glassy plastics refers to rigid, polymeric materials tested at temperatures below their glass transition temperature where molecular motion is frozen in. In addition, the influence of testing variables such as temperature and loading rate on the fracture toughness of these materials was evaluated. Finally, several different types of specimens recommended in the literature for obtaining fracture toughness data were compared using glassy plastics as a test material.

II. THEORY

A complete review of fracture mechanics is beyond the scope of this paper and is unnecessary because of the numerous reviews available. For example, the recent review of the ASTM[4] contains good summaries of both the theory and experimental applications of this subject. However, some basic concepts of the fracture mechanics of linear elastic structures are presented here to aid the discussion.

Fracture mechanics of linear elastic structures attempts to predict the conditions in which a structure loaded well below the general yield load will fail by rapid propagation of an existing crack. Since crack propagation can be considered as the movement of a single crack front through the body, attention is focused on the deformation and stresses near the crack tip. The deformation around a crack tip can be divided into three basic types depending upon the directions of the displacements of the crack surfaces. The opening mode (Mode I) is associated with crack displacements normal to the plane of the fracture; the edge sliding mode (Mode II) considers shear displacements of the crack surfaces perpendicular to the leading edge of the fracture; and the screw sliding mode (Mode III) is characterized by shear displacements of the crack surfaces parallel to the leading edge. Since the overall stresses are assumed to be within the elastic range of the structure, the stresses around the crack are calculated by ordinary elasticity theory. Very close to the crack tip, the stresses obtained from elasticity become so large that plasticity or other nonlinear effects become important. Thus, the solution of an elastic-plastic problem is actually required but such a solution is not

available. It is assumed, therefore, that the elastic solution can be applied except in the immediate neighborhood of the crack tip and that the inelastic region is small. The elastic-plastic problem is thus approximated by a crack in an elastic medium whose size is increased by the presence of the inelastic region.

Although the exact mathematical form depends upon the geometry of the structure and the loading, it is found that in the neighborhood of a crack, the stresses, σ_{ij}, associated with a specific mode of deformation have the form:

$$\sigma_{ij} = \frac{K}{\sqrt{2\pi r}} f_{ij}(\theta) \qquad (1)$$

where r, θ are polar coordinates centered at the crack tip; $f_{ij}(\theta)$ is dependent upon the particular stress component but not on the specimen geometry or applied load and K is called the stress intensity factor which is the same for all stress components. Only the parameter K relates the local stresses to the applied load and geometry of the specimen. As defined, the parameter K defines the local stress level in the neighborhood of the crack and increases with increasing load much like the stress in a tensile specimen increases as the applied load increases. Specific mathematical forms for K for various loading conditions and geometries have been calculated and an exhaustive tabulation is given by Paris and Sih.[8] For example, for a very large plate containing a small central crack of length 2a and loaded in tension by the stress σ normal to the crack,

$$K = \sigma(\pi a)^{1/2}.$$

The criteria of fracture can be obtained in several different but equivalent ways. One can assume that fracture occurs when a local stress or some combination of local stresses reaches a critical value. Since the stress intensity factor is common to all stress components and is the only parameter which depends on the applied loading, this is equivalent to assuming a critical value of $K = K_{crit}$ at fracture. The relationship of K_{crit} to the applied K at fracture is analogous to the relation of the yield strength to the applied stress at yield. The applied stress and K values are mechanics concepts dependent upon the loading and specimen geometry. The yield stress and K_{crit} are supposedly material properties dependent upon such variables as temperature, strain rate and microstructure. However, K_{crit} is found to depend upon specimen thickness and to a lesser extent specimen size. These effects are rationalized on the basis of their effect on the size and nature of the inelastic region adjacent to the crack tip.

An alternate approach to a fracture criteria is to consider an energy balance analogous to the original work of Griffith. Specifically, one notes that as a crack propagates, the elastic strain energy stored in a structure decreases. The released strain energy is assumed to be used in the production of the fracture surfaces and associated inelastic regions; energy may also be added or subtracted from the specimen by the loading system. Unstable, fast fracture is assumed to occur when the rate of release of elastic strain energy is greater than the rate of absorption, i.e., fracture occurs for a critical value of the strain energy release rate.

Irwin[9] first noted that the strain energy released when a crack extended a short distance had to equal the work that would be required to reclose this crack extension provided no work is done by the loading system. This work involves the stresses and displacements around the crack tip and Irwin, using relations such as Eq. (1) was able to show, for Mode I deformation:

$$K_I^2 = EG_I \quad \text{for plane stress} \tag{2a}$$

$$(1-\nu^2)K_I^2 = EG_I \quad \text{for plane strain} \tag{2b}$$

where E is Young's modulus, ν is Poisson's ratio and G_I is the strain energy release rate. Several authors[8] have shown the strain energy release rate is independent of the assumption that no work is done by the loading system so that Eq. (2) is completely general. The equivalence of a critical strain energy release rate (Griffith's approach) or a critical stress intensity factor (fracture mechanics approach) is shown by Eq. (2).

The conditions of plane strain and plane stress used in Eq. (2) refer to idealized states of stress defined to simplify the mathematical description of the stresses near the crack. Physically, these states of stress refer to two limiting degrees of restraint of deformation in the thickness direction. Plane stress considers no restraint in the thickness direction and is associated with thin sheets while plane strain considers complete restraint (no deformation) in the thickness direction and is associated with thick sheets. Thick specimens generally fracture with a flat, Mode I surface and K_{crit} is almost independent of specimen size and is usually written K_{Ic} (and G_{Ic}). Thin specimens frequently show an oblique, 45° shear fracture most likely associated with more than one mode of fracture

(mixed mode); K_{crit} depends strongly on specimen size for this case and is written K_c (and G_c). The term, fracture toughness, is often used in the place of either K_{crit} or G_{crit} values when discussing the fracture resistance of materials. In this report fracture toughness refers only to K_{Ic} values.

The above discussion applies to a cracked specimen of any material provided that the majority of the specimen is in a range in which the material exhibits a primarily linear elastic response. This condition applies for glassy plastics as well as metals provided the applied stresses are well below the yield stress. Since the inelastic region is not directly considered in the mechanics of the problem, the difference in the mechanism of the inelastic response for metals and glassy plastics does not have to be considered.

The experimental determination of K (or G) values usually follows one of two approaches. One technique utilizes a specimen with a machined crack and loading condition for which a mathematical relation for K is known. By measuring the applied nominal stress and the crack length at the onset of rapid crack propagation, one can calculate K_c. Another approach, and the one primarily used for this work, was that developed by Irwin and Kies[10] which relates the change in elastic compliance of the specimen during crack propagation to the strain energy release rate, G. Specifically,

$$G = \frac{P^2}{2B}\left(\frac{dc}{da}\right) \qquad (3)$$

where P is the applied load, B is the thickness, a is crack length and c is the compliance (extension of the specimen per unit load). Alternately, in terms of the stress intensity factor, K, for the case of plane strain:

$$\frac{2K^2(1-\nu^2)WB^2}{P^2} = \frac{d(ECB)}{d(a/w)} \qquad (4)$$

Here ν and E are Poisson's ratio and Young's modulus respectively. The compliance of a specimen with a narrow machined notch is measured as a function of notch length. The right hand side of Eq. (4) is then obtained by graphically or numerically differentiating the compliance curve. Equation (4) is in dimensionless form and hence applies to all specimens geometrically similar to the calibration specimen and is independent of material. In order to determine a value of K_c, one observes the load and crack length at the onset of rapid crack propagation. From the crack length, a value of the right hand side of Eq. (4) is obtained which, with the applied stress σ, allows K_c to be calculated. Detailed suggestions of testing including requirements for test specimens, and methods of measuring crack length are described in Ref. 11.

III. EXPERIMENTAL

A. Materials

The materials selected for this investigation are listed in Table I. Sufficient material was purchased to allow all specimens of a given material and thickness to be machined from a single sheet or rod. The materials were selected to represent different classes of rigid glassy, thermoplastics. The thickness of the sheet was chosen to enable values of K_{Ic} to be obtained based on the results of preliminary screening tests.

B. Test Program

The program of testing can be divided into four parts by test objective:

1. Specimen Design

The correlation between the values of K_{Ic} measured with different specimen types was investigated using 1 × 2 inch single edge notch (SEN) specimens (Fig. 1a), 3 × 12 inch center notch (CN) specimens (Fig. 2a) and notched round bars (Fig. 2b). Sheet specimens were prepared from polycarbonate (1/4 inch thickness), and acrylic (1/8 inch); the notched round specimens from 1/2 and 1-1/16 inch polycarbonate rod. These tests were performed at room temperature (300°K) at a cross head speed of 0.2 cm/min (0.08 in/min).

2. Size Effects

The effects of specimen thickness on fracture toughness of plastics was investigated by testing 1 × 2 in SEN polycarbonate specimens of various thicknesses. Four methods of attaining thicker specimens were

evaluated; as extruded sheet, milled to thickness from 5/8 inch sheet, laminated to thickness from 1/16 inch sheets, and laminated to thickness from 1/8 inch sheets. Solvent cementing (ethylene dichloride) was used for the lamination. The nominal thicknesses investigated were:

as extruded:	1/16, 1/8, 3/16, 1/4, 3/8, 1/2, 5/8
milled:	1/8, 1/4, 3/8, 1/2
laminated (1/16 sheets):	1/4, 3/8, 1/2
laminated (1/8 sheets) :	1/4

The effect of specimen length was evaluated using SEN specimens from polycarbonate (1/4 inch thick) and acrylic (1/8 inch thick) with dimensions 1x4, 1x8, 1x12 inches. Additionally 2x4 SEN specimens of polycarbonate were tested. These specimens are geometrically similar to the 1x2 SEN specimens and were tested to confirm the dimensionless nature of the calibration procedure. This series of tests was performed at room temperature (300°K) with a cross head speed of 0.2 cm/min (0.08 in/min).

3. Temperature, Strain Rate

The effect of test temperature and strain rate on the fracture toughness of polycarbonate (1/4 in. sheet) and acrylic (1/8 in. sheet) was investigated using 1x2 SEN specimens. At a constant cross head speed of 0.2 cm/min (0.08 in/min), specimens were tested at 75, 50, 25, 0, -50, -100, -150°C (348, 323, 298, 273, 223, 173, 123°K). At room temperature (300°K) cross head speeds of 5, 0.2, and 5×10^{-3} cm/min (2, 0.08, 2×10^{-3} in/min) were evaluated.

4. Material

The fracture toughness of four commercial plastics was determined using 1x2 SEN specimens; polycarbonate (PC), polystyrene (PS), acrylic (A),

and vinyl chloride-vinyl acetate (VCA). All tests were performed at room temperature (300°K) and a cross head speed of 0.2 cm/min (0.08 in/min).

5. Tensile Tests

Tensile tests were performed on specimens with a gage length two inches long, 0.250 inches wide and 0.125 inches thick. The tests were performed at room temperature (300°K) and a cross head rate of 0.2 cm/min (0.08 in/min). A strain gage extensometer was used for the initial portion or the load-elongation record for PC and A.

C. Procedure

Prior to testing all specimens were conditioned at 23°C and 50 percent relative humidity in accordance with Procedure A of ASTM D618. All testing was done in an Instron testing machine of 5000 kg capacity. Low temperature tests were performed in an atmosphere of cooled nitrogen vapor[12] as shown in Fig. 3b. Elevated temperature tests were conducted with a closed cycle warm air system in which the air is heated during passage through copper coils in an oil bath (Fig. 3a). The test temperature was measured and controlled by thermocouples attached to the specimens.

The machined notches in the SEN specimens were terminated in a razor cut about 0.020 in. deep. Figure 1b shows a typical crack tip configuration. The notches in the CN and notched round specimens were used as-machined. Both the SEN and CN specimens were pin loaded but the CN specimens had mild steel reinforcing plates bolted to the specimens to prevent tear out by the loading pins. The notched round specimens were loaded through threaded collars.

D. Analysis

The calculation of K_{Ic} values requires the load and crack length at the onset of fast fracture. For the plastics tested in this work, the load-crosshead displacement curves were either of the catastrophic fracture type (Fig. 4) or the pop-in type (Fig. 5). The pop-in curve occurs when a flat, mode I fracture is initiated at the machined notch but is arrested by high energy, shear deformation developing after the initial fracture. Specifically, the mode I fracture propagates most rapidly in the center of the specimen where a triaxial tensile stress condition exists thus forming a semi-circular crack front. This crack front is bounded by thin regions near the plate surface which deform by shear as the crack propagates and thus arrest the crack.

The 1/4 inch thick polycarbonate specimens appeared to be on the borderline between the two types of fracture behavior since both types were observed under identical testing conditions. The curves of Figs. 4 and 5 are the load-displacement records of two such specimens. The maximum load for the catastrophic case is almost identical to the pop-in load for the other specimen. This justifies the use of the pop-in load to calculate K_{Ic}. Thus, the load at fracture was taken either as the pop-in load or the maximum load for catastrophic failure. For either case, the fracture toughness values obtained are assumed to represent plane strain conditions.

It was assumed that little crack extension took place prior to fast fracture. This assumption was based on the linearity of the load displacement curves up to fracture (or pop-in) and visual observations of the crack tip. Because of the transparency of the plastics being tested and the high reflectivity of internal surfaces, the crack tip was readily

visible during testing and little crack growth prior to fracture or pop-in was observed. However, the occurrence of pop-in was observed to be accompanied by a rapid but limited extension of the crack. Thus, the crack length at fracture was taken to be the initial crack length and was measured on the fractured specimens with a traveling microscope. However, as noted in the Theory Section, the effect of the inelastic region is taken into account by an increase in effective size of the crack. Irwin and McClintock[13] have estimated the radius of the plastic zone for plane strain conditions as:

$$r_y = \frac{1}{4\pi(2)^{1/2}} \left(\frac{K_{Ic}}{\sigma_y} \right)^2 \qquad (5)$$

where σ_y is the yield stress. This value of the plastic zone size is used to increase the measured crack length and thus obtain a value of K_{Ic} corrected for inelastic effects. Since the plastic zone radius depends on K_{Ic}, an iterative procedure is required which usually involves only one iterative step. The calculation K_{Ic} for each type of specimen is outlined below.

1. SEN Specimens

K_{Ic} values were calculated using the calibration curve shown in Fig. 7. This curve was obtained with calibration specimens of polystyrene and SAE 4340 steel.[14] The experimental results of Sullivan[15] and the theoretical curve of Gross and Srawley[16] are included for comparison. The same calibration curve was used for all SEN specimens independent of length. The values of K_{Ic} measured at room temperature and normal loading rate (0.2 cm/min) were corrected for plastic zone size by increasing the measured crack length by an amount r_y. This correction amounts to about 3 percent

increase in K_{Ic} for PC, PS, and VCA and no increase for acrylic. The K_{Ic} values measured at other temperature and strain rates were not corrected since tensile tests were not performed at these conditions to obtain σ_y. However, estimates of the correction using tensile data from the literature indicates the maximum correction would be about 6 percent for PC and 3 percent for acrylic.

2. CN Specimens

The theoretical curve relating K_{Ic} and the applied load and crack size for CN specimens shown in Fig. 5 of Ref. 11 was used to obtain K_{Ic} values. These values were corrected for plastic zone size effects by increasing the measured crack total length by $2r_y$.

3. Notched Round Specimens

The theoretical curve relating K_{Ic} to the applied load and notched diameter for notched round specimens shown in Fig. 9 of Ref. 11 was used to obtain K_{Ic} values. The values were corrected for plastic zone size effects by decreasing the notched diameter by $2r_y$.

IV EXPERIMENTAL RESULTS

The results for all tests are summarized in Table II which includes the test conditions, specimen details, fracture mode, and range of toughness values observed. For convenience, the values applicable to specific test objectives are presented in separate tables or figures. The fracture toughness of the four plastics investigated in this work are listed in Table III along with values of the yield strength, modulus, plastic zone size, strain energy release rate and effective surface energy. Table IV displays the fracture toughness values obtained for PC and A using different specimen geometries and sizes. Table V shows the effect of specimen thickness on the fracture toughness of PC. The effect of temperature and strain rate on the fracture properties of PC and A are shown in Figs. 8, 9, and 10.

The macroscopic classification of the observed fracture surface characteristics is outlined in Table II. As noted previously, the specimens failed in either an abrupt fracture or a pop-in type. The abrupt, catastrophic fracture leads to a flat fracture surface with little or no shear lips. The pop-in mode has a flat central region associated with pop-in surrounded by shear lips formed primarily after pop-in. Typical flat fractures are shown in Figs. 11-13 for A, PS, and VCA, respectively. Both modes of fracture were observed with PC depending upon the thickness, method of fabrication and test conditions. Figure 14 shows a specimen which fractured in the pop-in mode; a flat fracture is shown in Fig. 15. The effects of temperature and strain rate on the fracture appearance of PC and A are shown in Figs. 16-31. The view in Figs. 11-31 is normal to the fracture surface; the direction of crack

propagation is from left to right in the macrograph and from top to bottom in the micrographs.

The microscopic features of the fracture surfaces exhibit considerable variety depending upon the material, test condition, and specimen geometries. Typical features are shown in Figs. 11-31. It is emphasized that these features were reproducibly developed as a function of material and test condition. In general, two or more regions are clearly delineated. The first area adjacent to the razor cut notch is the fracture initiation region and hence associated with slow crack growth. This area is either flat as with PS or has widely spaced, shallow furrows as with PC. The surface is relatively smooth in either case although some fine lines and small parabola markings do appear. Because of its smoothness, this area is usually highly reflective and is often called the mirror area. This first region is shown in the middle view of Figs. 11-31.

The second region, which is separated from the first by a sharp transition, corresponds to a fast crack growth region and is shown in the lower view of Figs. 11-31. Several types of features can be identified in this region. The PC shows many well defined parabola markings especially the specimens machined from the 0.675 inch plate. Both the PS and VCA show a very coarse "cobble-stone" pattern in this area while the acrylic surface is very flat and shows a very fine pattern. Evidence of color patterns on the fracture surface was observed with all materials but such patterns were more developed and extensive on acrylic specimens.

Significant variations in the macroscopic and microscopic features of the fracture surfaces were observed by varying test temperature. With PC, the majority of the fractures were the abrupt, flat mode at both low and

elevated temperatures with the pop-in mode and larger shear lips being observed at intermediate temperature (-50 to 25°C) (223 to 290°K). The surfaces of the specimens tested at intermediate temperatures showed long tear lines along the fracture trajectory with a smooth region between the lines. At low and elevated temperatures, the fracture surfaces exhibit groups of uniformly spaced ribs of varying characteristics. At low temperatures, the ribs formed somewhat of a herringbone pattern while at elevated temperatures, the ribs were straighter and smaller.

The surface features of the acrylic specimens also varied with temperature. At elevated temperature, the surface was smooth with some fine lines parallel to the crack trajectory. At low temperatures, parabola markings became prominent especially in the range -100 to -50°C (173 to 223°K). For both PC and A, it was noted that a mirror region of approximately the same structure appeared at all temperatures although its size varied.

At high strain rates, the fracture surface of PC was very similar to the low temperature specimens except the ribs appeared associated with a single fracture origin starting as concentric semi-circles and expanding into straight lines away from the origin. At high strain rates, the acrylic showed fine tear lines along the crack trajectory.

V. DISCUSSION

This section will be broken into sections to facilitate discussion of the numerous phases of the program.

A. Test Procedure

Several authors have proposed criteria to be used in determining if a specimen size was large enough to yield an acceptable value of plane strain fracture toughness. The two main objectives of these criteria are to assure enough thickness constraint to provide a plane strain condition and to assure that the inelastic region is small so that the stresses around the crack are adequately described by elasticity. Generally, these requirements specify the minimum size of the specimen in terms of the plastic zone radius, r_y. The criteria proposed for sheet specimens for the minimum ratio of thickness-to-plastic zone radius are 11.3,[17] 14,[18] and 44.4.[11] These values have been modified from the original papers by using Eq. (5) for the plastic zone radius rather than the other forms originally used so that a consistent comparison could be made. As Table III shows, the standard thickness specimens used in this work meet the first two criteria but not the most conservative except for acrylic. However, since either abrupt fractures or distinct pop-ins were obtained for all specimens used in this study, it is considered that the thicknesses are adequate. In the testing of PC, it was observed that a pop-in could be observed down to a thickness of about 0.080 inches which corresponds to $B/r_y = 10$ which is close to the value proposed by Hahn and Rosenfield.[18] The transparency of the plastics can also be used to confirm the adequacy of the specimen thickness. Figure 6 shows an end-on

view of the crack in a pop-in specimen at various loads. This figure shows that extensive plastic zones do not develop until after pop-in for the 0.250 inch thick PC specimens.

For notched round specimens, Brown and Srawley[11] recommend a diameter four times the thickness of a sheet specimen. The round specimen used in this study again meets this requirement with the first two thickness criteria but not the third. The recommendations for other dimensions given by Brown and Srawley[11] can be summarized as follows (in terms of minimum acceptable thickness for convenience):

Specimen	Crack Length	Width (diam.)	Length
SEN	1	2	8
NR	1	4	16
CN	2	4	16

The specimens used in this study meet these recommendations using the first two thickness criteria but not always the third.

In addition to these size limitations, it is usually assumed that the ratio of the applied nominal stress to the yield stress must be less than 0.8 for a valid test with a sheet specimen.[19] The nominal stress for these specimens is defined as the stress at the tip of the crack including both bending and direct tension but not including stress concentration effects of the notch.[20] The ratio is tabulated in Table III for the SEN sepcimens and it is seen that this requirement is met. Similarly, the center notch specimens can be shown to meet this requirement. For the notched round specimens, the allowable ratio is increased to 1:1[19] and on this basis the 1-1/16 rod meets the requirement while the 1/2 rod has a ratio slightly in excess of the allowable value (1.25).

B. Material

From the values shown in Table III, it appears that while PC is a tough plastic, it does not have a greater fracture toughness than the VCA copolymer. In addition, the difference between high toughness PC and the low toughness A or PS is less on the basis of strain energy release rate than on the basis of impact strength. However, at room temperature the VCA, A, PS specimens with a thickness of 0.125 inches consistently fracture in the flat, abrupt mode while the thicker (0.250 inches) PC usually exhibited a pop-in type of failure developing extensive shear lips and tearing after pop-in. Thus, the toughness advantage of PC relative to other glassy plastics is that the flat mode of fracture becomes unstable and converts to a shear mode for thicker sheets and not that PC has an inherently greater resistance to propagation of a flat crack.

The values of effective surface energy for PS and A obtained in this work show adequate agreement with the values obtained by other workers and other methods as shown in Table VI.

C. Temperature

The effects of temperature on fracture toughness of A and PC produced some interesting results as shown in Figs. 8 and 9, which include values of impact strength and effective surface energy (for acrylic). The increase in toughness exhibited at low temperature for both PC and A is not expected based on work with metals and especially for a material exhibiting a sharp ductile-brittle transition like PC. However, the increasing toughness for acrylic does correspond to the increase in effective sur-

face energy in the same temperature range reported by Berry.[21] Berry attributes this increase to decreased segmental mobility of the polymer chains at low temperature increasing the energy to produce inelastic effects near the fracture surface. However, Berry did not observe any leveling off of the surface energy at temperatures as low as 78°K whereas the fracture toughness of acrylic appears to level off and perhaps decrease below 220°K. Also the impact strength of acrylic is reported to remain almost constant over the range 210 to 350°K which does not correlate with the fracture toughness results.

The occurrence of a minimum toughness near 223°K for PC closely corresponds to the ductile-brittle transition for this material. The behavior below the minimum is similar to acrylic and may also be due to decreasing segmental mobility. One is tempted to attribute the increase in toughness above the minimum to a change in fracture mode with greater ductility and larger shear lips as is observed with the impact results. However, the results of this work do not substantiate this approach since a greater incidence of flat, abrupt type fractures was observed at 323 and 348°K than at room temperature. At 373°K, the specimens showed extensive deformation and neither a pop-in nor a flat fracture were obtained.

To explain these results, it is noted that there are two mechanisms producing energy absorption in a flat fracture without extensive shear lips. The first involves increasing the surface area by developing extensive fracture markings; the absorbed energy includes not only the increase surface energy but also the energy involved in forming the markings usually by a tearing action to connect secondary fractures on slightly different levels. The importance of this mechanism can be estimated by

observing the density and size of the markings on the fracture surface. A second mechanism involves the formation of an inelastic zone along the crack surfaces. The energy absorbed in this mechanism depends on both the depth of the inelastic zone and on the specific energy of the processes involved.

The fracture surfaces of the acrylic (Figs. 16-21) and PC (Figs. 22-27) correlate well with toughness behavior having a higher density of coarse markings at low temperatures. The decrease in toughness at 273°K for A and 223°K for PC corresponds to the development of smoother fracture surfaces. An increase in toughness at elevated temperature may be due to energy absorption by formation of an inelastic zone. As noted, Berry[21] pointed out that the specific energy of the inelastic processes should decrease with increasing temperature due to increased segmented mobility. However, the depth of the inelastic zone should increase with increasing temperature for the same reason. Thus, the energy absorption in the formation of an inelastic zone may show increases at both high and low temperatures as long as other mechanisms do not prevent a flat fracture. Hence, at 323 and 348°K flat, brittle fractures or pop-in fractures were obtained with large toughness values but at 373°K, other deformation mechanisms appear to predominate. Examination of Fig. 8 shows a small increase in toughness for acrylic at 323°K. This may correspond to a process similar to PC but which is less developed since the glass transition temperature for acrylic is lower (105°C for acrylic compared to 150°C for PC).

D. Strain Rate

Increasing the strain rate in a tensile test of glassy plastics leads to an increase in strength and a decrease in ductility which is similar to the response to a reduction in temperature in a tensile test. However, this correspondence between increasing strain rate and decreasing temperature does not hold well for fracture behavior. For acrylic specimens, the fracture toughness decreased by increasing the loading rate from 0.2 to 5 cm/min (0.08 to 2 in/min) whereas an increase in toughness was observed with decreasing temperatures. In addition, the fracture surfaces of the acrylic specimens tested at high loading rate (Fig. 29) more closely resembled the smooth, elevated temperature surfaces than the coarser low temperature fractures. For PC, the fracture surfaces at increased loading rates corresponded more closely to the coarse, lower temperature surfaces. The decrease in toughness for acrylic occurred at a loading rate somewhat greater than 0.2 cm/min (0.08 in/min), which compares well with a sharp decrease in tensile energy to failure for acrylic observed by Maxwell and Harrington[23] at about 0.5 cm/min.

Considering the discussion of the mechanisms of energy absorption in Section C, it appears that the most likely explanation for this behavior is a reduction in the depth of the inelastic zone. This reduction would be produced when the rate of loading exceeded the basic relaxation times of the viscous mechanisms involved in the inelastic zone. This same mechanism is responsible for the decrease in ductility observed in high strain rate tensile tests.

E. Thickness

Based on results with metals, thin sheets are expected to fail in an oblique shear mode (plane stress) with high energy absorption while thick sheets usually exhibit a flat tensile mode (plane strain) with lower energy absorption. The fracture toughness for plane strain conditions is found to be almost independent of thickness. As discussed above, the pop-in mode is assumed to correspond to a local plane strain condition at the moment of fracture initiation and since all data in this work were obtained with either pop-in or flat fractures, thickness should not be an important parameter. Examination of Table V shows this to be partially substantiated. For the as-extruded PC sheet materials, only the thinnest (0.080 inches) and the thickest (0.625) show a significant variation. The increase for the thin sheet is probably a result of pop-in being almost suppressed at this thickness and thus appreciable shear deformation was associated with pop-in. The high value of toughness for the 0.675 inch sheet may be due to a subtle variation in the processing of thin sheets and thick sheets. Several results lend support to the conclusion that the thicker sheet had different properties from the thin sheet independent of thickness effects. The toughness of the 0.125 and 0.250 inch specimens milled from the 0.675 sheet agree very well with the thick specimens. In addition, the fracture surfaces of all PC specimens machined from the thick sheet exhibited a much higher density of parabola markings than the fracture surfaces of as-extruded sheets of comparable thickness. This implies that the thick sheet material contained a higher density of sites for initiation of secondary fractures.

F. Method of Fabrication

One objective of this program was to compare the effect on toughness of obtaining a specified thickness by various means including as-extruded sheet, milled to thickness from a thick sheet, and lamination of thin sheets. This latter technique was included since this is the procedure recommended by ASTM standard D256-56 for impact testing of thin plastic sheets. As noted above, the milled PC specimens are considered to represent a different level of toughness because the thicker sheet had a larger inherent toughness. Thus, no conclusion could be reached on the effect, if any, of milling to thickness. The results of Table V do show a significant increase in toughness for the laminated specimens. The PC specimens laminated to a thickness of 0.250 inches from 0.125 inch sheet had a fracture toughness of 3.97 ksi $(in)^{1/2}$ while the 0.125 inch sheet used for lamination had a toughness of only 3.41 ksi $(in)^{1/2}$. For these laminated specimens, it was observed that the laminated interfaces exhibited considerable crazing in the neighborhood of the crack tip. In fact, the crazed regions had the shape predicted for plastic zones at the tip of a crack. The higher toughness is probably due to the energy absorbed in this crazing process. This conclusion is supported by the higher fracture toughness obtained with the specimens laminated from 1/16 inch sheet than from 1/8 inch sheets since these specimens have an increased number of bonding interfaces. These observations conflict with the results of Kaufman[24] on adhesive bonded aluminum sheets in which he observed that the plane strain fracture toughness was independent of bonding and number of bonding layers. This difference probably is due to the nature of the bonding layers. The increase in toughness observed for the laminated plastics may be of

significance in interpreting impact results from similar specimens since it indicates that laminated specimens tend to over-estimate the fracture properties of the sheet material..

G. Specimen Geometry

The fracture toughness values obtained with the center notch and notched round specimens, while somewhat higher, show adequate agreement with the small SEN specimens and very good agreement among themselves. The higher values of toughness observed with these specimens probably results from the larger crack tip radius with the specimens since they were tested with as-machined notches. Similar increases were observed with several small SEN specimens inadvertently tested without sharpening the notch with a razor blade.

The SEN specimens show a general increase in toughness with increasing length except for the 1×4 acrylic specimens. This result may be due to the effect on specimen length on eccentricity of loading. As Srawley et al.[25] noted, the eccentricity tends to decrease as the specimen length increases due to bending effects. The numerical results of Gross and Srawley[16] predict a decrease in stress intensity factor with a decrease in eccentricity for a given crack length, thus indicating that the stress intensity factor should decrease with increasing length. Since the calibration curve for short 1×2 specimens was used to calculate toughness of the larger specimens as well, the toughness of these specimens is expected to be over-estimated. The angle of bending necessary to account for the variation in toughness can be estimated using the results of Gross and Srawley and is found to be from 1 to 2° except for two of the 1×4 acrylic specimens which appears

to be a reasonable value. Figure 32 shows that the photoelastic pattern observed for each specimen length was similar, demonstrating that the stress distribution in the SEN specimen does not depend strongly on length.

H. Fracture Topography

The effects of the variables studied in this program on the macro and micro appearance of the fracture surfaces have been discussed above. Several reviews[22,26-28] of fracture topography of polymeric materials are available in the literature in which possible mechanisms for the formation of the observed features are discussed. These mechanisms usually involve the initiation and growth of secondary fractures on several levels ahead of the main crack interface due to the stress concentration of the main crack. The intersection of the various crack systems forms the observed fracture traces. For parabola markings, the point of initiation of the secondary crack should appear at the focus as is clearly shown in Fig. 33.

The changes in topography in different regions is usually attributed to variations in crack velocity. However, other than this qualitative observation, the mechanisms producing different morphologies and the effect of such variables as temperature and strain rate are not well understood.

VI. CONCLUSIONS

The principal conclusions of this work can be summarized as follows:

1. Fracture mechanics is useful for evaluating the fracture behavior of glassy plastics in a manner similar to that currently used for metals.

2. The fracture toughness of glassy plastics decreases with increasing load rate especially at high rates (greater than 1 cm/min).

3. The fracture toughness of glassy plastics is very sensitive to test temperature. Increases of toughness at low temperatures were observed for both PC and acrylic. At elevated temperatures, a toughness increase is observed for PC. This behavior is attributed to variations in the thickness and specific energy involved in the formation of inelastic zones along the fracture surface.

4. Adequate agreement of fracture toughness values is obtained with specimens of different geometries.

5. Differences in topography of the fracture surface correspond closely to variations in fracture toughness; increased toughness being associated with a greater density of surface markings.

6. Fracture toughness defined by pop-in methods was almost independent of thickness and comparable to values obtained on thick specimens exhibiting abrupt fracture.

7. Laminated specimens have a higher fracture toughness which is probably due to crazing at the bonded interfaces.

8. Glassy plastics can be useful in fundamental studies of fracture mechanics. For example, the transparency of the plastics used in this

study allowed visual observation of the pop-in phenomena and the development of plastic zones around the crack.

ACKNOWLEDGMENTS

This work was supported by the United States Atomic Energy Commission. The comments of W. W. Gerberich on this report are greatly appreciated. One of the authors (PLK) gratefully acknowledges the support of an NSF Fellowship during the course of this work.

REFERENCES

1. G. R. Irwin, Fracture Dynamics, in Fracturing of Metals (American Soc. Metals, Cleveland, 1940), p. 147.

2. G. R. Irwin, Fracture Mechanics, in Structural Mechanics (Pergamon Press, London, 1960), p. 557.

3. G. R. Irwin and A. A. Wells, A Continuum-Mechanics View of Crack Propagation, Met. Rev. 10, 38 (1965).

4. Fracture Toughness Testing and Its Applications, (ASTM, Philadelphia, 1965).

5. A. S. Tetelman and A. J. McEvily, Fracture of Structural Materials (John Wiley and Sons, Inc., New York, 1967).

6. A. van der Boogaart and C. E. Turner, Fracture Mechanics: A Review of Principles with Special Reference to Applications for Glassy Plastics in Sheet Form, Plastics Institute Trans. and Journal 31, 109 (1963).

7. J. P. Berry, Brittle Behavior of Polymeric Solids, in Fracture Processes in Polymeric Solids, B. Rosen, Editor (John Wiley and Sons, Inc., New York, 1964), p. 195.

8. P. C. Paris and G. C. Sih, Stress Analysis of Cracks, in Fracture Toughness Testing and Its Applications (ASTM, Philadelphia, 1965), p.30.

9. G. R. Irwin, Analysis of Stresses and Strains Near the End of a Crack Traversing a Plate, J. Appl. Mech. 24, 361 (1957).

10. G. R. Irwin and J. A. Kies, Critical Energy Rate Analysis of Fracture Strength, Welding Journal, 33, [4], 193s (1954).

11. W. F. Brown and J. E. Srawley, Plane Strain Fracture Toughness Testing of High Strength Metallic Materials (ASTM, Philadelphia, 1967).

12. E. T. Wessel and R. D. Olleman, Apparatus for Tension Testing at Subatmospheric Temperatures, ASTM Bull. 187, 56 (1953).

13. F. A. McClintock and G. R. Irwin, Plasticity Aspects of Fracture Mechanics, in Fracture Toughness Testing and Its Application (ASTM, Philadelphia, 1965), p. 84.

14. Y. Katz, P. L. Key and E. R. Parker, Dimensionless Fracture Toughness Parameters, University of California, UCRL Report, UCRL-17895.

15. A. M. Sullivan, New Specimen Design for Plane-Strain Fracture Toughness Tests, Mat. Res. and Stand. 4, (1), Jan. 1964, pp. 20-24.

16. B. Gross and J. E. Srawley, Stress-Intensity Factors for Single-Edge-Notch Specimens in Bending or Combined Bending and Tension by Boundary Collocation of a Stress Function, NASA TN-D-2603, Jan. 1965.

17. R. W. Boyle, A. M. Sullivan and J. M. Krafft, Determination of Plane Strain Fracture Toughness with Sharply Notched Sheets, Welding Journal, 41, (428s), 9, (1962).

18. G. T. Hahn and A. R. Rosenfield, Sources of Fracture Toughness: The Relation Between K_{Ic} and the Ordinary Tensile Properties of Metals, Presented at ASTM Symposium on Applications Related Phenomena in Titanium and Its Alloys, Los Angeles, 1967.

19. Progress in Measuring Fracture Toughness and Using Fracture Mechanics, Mat. Res. and Stand. 4, (107), 3 (1964).

20. J. E. Srawley and W. F. Brown, Fracture Toughness Testing Methods, in Fracture Toughness Testing and Its Applications (ASTM, Philadelphia, 1965), p. 133.

21. J. P. Berry, Fracture Processes in Polymeric Materials, IV: Dependence of the Fracture Surface Energy on Temperature and Molecular Structure, J. Polymer Sci. A1, 993 (1963).

22. I. Wolock and S. B. Newman, Fracture Topography, in Fracture Processes in Polymeric Solids, B. Rosen, Editor (John Wiley and Sons, Inc., New York, 1964), p. 235.

23. B. Maxwell and J. P. Harrington, Effect of Velocity on Tensile Impact Properties of Polymethyl Methacrylate, Trans. ASME 74, 579 (1952).

24. J. G. Kaufman, Fracture Toughness of 7075-T6 and T651 Sheet, Plate, and Multilayered Adhesive-Bonded Panels, J. Basic Eng. 89, (3), 503, (1967).

25. J. E. Srawley, M. H. Jones, and B. Gross, Experimental Determination of the Dependence of Crack Extension Force on Crack Length for a Single-Edge-Notch Tension Specimen, NASA TN-D-2396, 1964.

26. J. A. Kies, A. M. Sullivan, and G. R. Irwin, Interpretation of Fracture Markings, J. Appl. Phys. 21, (7), 716 (1950).

27. I. Wolock, J. A. Kies, and S. B. Newman, Fracture Phenomena in Polymers, in Fracture, B. L. Averbach. Editor (M.I.T. Press, Cambridge, 1959), p. 250.

28. Ir. J. Leeuwerik, Kinematic Features of Brittle Fracture Phenomenon, Rheologica Acta 2, (1), 10, (1962).

29. J. J. Benbow and F. C. Roesler, Experiments on Controlled Fractures, Proc. Phys. Soc. (London) B70, 201 (1957).

30. N. L. Svensson, The Variation of the Fracture Energy of Brittle Plastics with Temperature, Proc. Phys. Soc. (London) 77, 876 (1961).

31. J. P. Berry, Determination of Fracture Surface Energies by the Cleavage Technique, J. Appl. Phys. 34, (1), 62 (1963).

32. J. P. Berry, Fracture Processes in Polymeric Materials. I. The Surface Energy of Polymethyl Methacrylate, J. Polymer Sci. 50, 107 (1961).

33. J. R. Hyndman, The Impact Behavior of Rigid PVC Compounds, Polymer Eng. and Sci. 6, (2), 169 (1966).

34. Technical Data on Plastics, (Plastic Materials Manufacturers Association, Inc., May 1948).

35. L. E. Nielson, Mechanical Properties of Polymers, (Reinhold Publ. Co., New York, 1962).

36. J. C. Kulpinsky, Union Carbide, private communication.

37. L. J. Broutman and F. J. McGarry, Fracture Surface Work Measurements on Glassy Polymers by a Cleavage Technique I. Effects of Temperature, J. Appl. Polymer Sci. 9, 589 (1965).

Table I. Materials and product dimensions

Material	Specification	Sheet Thickness (in.)	Rod Diam. (in.)
Polycarbonate	-	0.080, 1/8, 3/16, 1/4 3/8, 1/2, 5/8	1/2, 1-1/16
Polystyrene	Mil-P-77C Type E2	1/8	-
Acrylic	Mil-P-5245	1/8	-
Vinyl chloride-vinyl acetate	L-P-535 Comp. B Type I-Grade B	1/8	-

Table II. Summary of fracture toughness tests

Material (1)	Specimen Geometry	Nominal Thickness (in.)	Test Conditions: Temp. °C	Test Conditions: Crosshead Rate cm/min	Number of Specimens	Average K_{Ic} ksi(in.)$^{1/2}$	Range of Values: + ksi(in.)$^{1/2}$	Range of Values: − ksi(in.)$^{1/2}$	Mode of Fracture (2)
PS	1X2 SEN	0.125	RT	0.2	4	1.64	0.06	0.03	F
VCA	1X2 SEN	0.125	RT	0.2	5	3.71	0.05	0.09	F
A	1X2 SEN	0.125	RT	0.2	4	0.99	0.07	0.06	F
A	1X4 SEN	0.125	RT	0.2	3	1.41	0.13	0.21	F
A	1X8 SEN	0.125	RT	0.2	2	1.28	0.05	0.05	F
A	1X12 SEN	0.125	RT	0.2	3	1.51	0.09	0.07	F
A	1X2 SEN	0.125	RT	5	3	0.42	0.10	0.05	F
A	1X2 SEN	0.125	RT	$5X10^{-3}$	3	0.96	0.15	0.09	F
A	1X2 SEN	0.125	0	0.2	3	1.49	0.05	0.06	F
A	1X2 SEN	0.125	-50	0.2	3	2.46	0.16	0.10	F
A	1X2 SEN	0.125	-100	0.2	5	2.38	0.28	0.24	F
A	1X2 SEN	0.125	-150	0.2	3	2.03	0.15	0.12	F
A	1X2 SEN	0.125	50	0.2	3	1.30	0.26	0.17	F
A	1X2 SEN	0.125	75	0.2	4	0.84	0.01	0.01	F
A	3X12 CN	0.125	RT	0.2	4	1.21	0.28	0.34	F
PC	1X2 SEN	0.080	RT	0.2	6	4.00	0.37	0.35	PI-SL
PC	1X2 SEN	0.125	RT	0.2	2	3.41	0.01	0.01	PI-SL
PC(M)	1X2 SEN	0.125	RT	0.2	2	3.43	0.16	0.15	PI-SL
PC	1X2 SEN	0.185	RT	0.2	6	3.25	0.04	0.15	PI-SL
PC	1X2 SEN	0.250	RT	0.2	7	3.29	0.08	0.06	PI-SL
PC(M)	1X2 SEN	0.250	RT	0.2	5	3.57	0.09	0.15	PI-SL,F
PC(L16)	1X2 SEN	0.250	RT	0.2	3	4.10	0.15	0.09	PI-SL
PC(L8)	1X2 SEN	0.250	RT	0.2	5	3.97	0.28	0.16	PI-SL
PC(M)	1X2 SEN	0.375	RT	0.2	3	4.05	0.07	0.13	F

UCRL-17911

Table II. Continued

Material (1)	Specimen Geometry	Nominal Thickness (in.)	Test Conditions: Temp. °C	Test Conditions: Crosshead Rate cm/min	Number of Specimens	Average K_{Ic} ksi(in.)$^{1/2}$	Range of Values: + ksi(in.)$^{1/2}$	Range of Values: - ksi(in.)$^{1/2}$	Mode of Fracture (2)
PC(L16)	1X2 SEN	0.375	RT	0.2	1	4.45	-	-	PI-SL
PC(M)	1X2 SEN	0.500	RT	0.2	4	3.96	0.20	0.16	F
PC(L16)	1X2 SEN	0.500	RT	0.2	3	4.09	0.09	0.04	F
PC	1X2 SEN	0.625	RT	0.2	3	3.73	0.13	0.13	F
PC	1X2 SEN	0.250	RT	5	5	2.11	0.20	0.18	PI-SL
PC	1X2 SEN	0.250	RT	1	3	3.10	0.28	0.16	PI-SL
PC	1X2 SEN	0.250	0	0.2	3	2.65	0.09	0.11	F-SL
PC	1X2 SEN	0.250	-50	0.2	2	2.14	0.03	0.04	F-SL
PC	1X2 SEN	0.250	-100	0.2	2	3.73	0.05	0.05	F
PC	1X2 SEN	0.250	-150	0.2	3	3.55	0.09	0.07	F
PC	1X2 SEN	0.250	+50	0.2	3	3.84	0.21	0.26	F, PI-SL
PC	1X2 SEN	0.250	+75	0.2	3	3.48	0.22	0.36	F
PC	2X4 SEN	0.250	RT	0.2	3	3.71	0.11	0.23	F
PC	1X4 SEN	0.250	RT	0.2	3	3.48	0.29	0.18	F, PI-SL
PC	1X8 SEN	0.250	RT	0.2	2	3.68	0.14	0.14	F
PC	1X12 SEN	0.250	RT	0.2	2	4.13	0.08	0.08	F
PC	3X12 CN	0.250	RT	0.2	2	3.81	0.10	0.11	F
PC	NR	1/2 (dia)	RT	0.2	2	3.97	0.02	0.01	F
PC	NR	1-1/16 (dia)	RT	0.2	2	3.79	0.03	0.04	F

(1) PC(M) - milled specimen, PC(L16) - laminated from 1/16 sheets, PC(L8) laminated from 1/8 sheets

(2) F - flat, SL - shear lips, PI-pop-in type

UCRL-17911

Table III. Room temperature fracture properties of glassy polymers

Material	K_{I_c}(3) ksi(in.)$^{1/2}$	σ_y ksi	r_y(1) in.×10^3	$\frac{B}{r_y}$	$\frac{\sigma_{nom}}{\sigma_y}$	E ksi	G_{I_c} lb in./in.^{2}	γ'(2) ergs/cm^2×10^{-5}	Izod Impact Strength ft-lb/in.	Glass Transition Temperature °C
Polycarbonate	3.29	8.5	7.9	32	0.63	300	30.0	27.6	16[33]	150[35]
Acrylic	0.99	10.5	0.50	250	0.16	350	2.46	2.15	0.55[34]	105[35]
Polystyrene	1.64	4.8	6.3	20	0.62	450[34]	5.06	4.58	0.25 - 0.40[34]	100[35]
Vinyl chloride - Vinyl acetate	3.71	9.5	8.1	15	0.67	350[34]	32.7	30.1	0.40 - 0.75[34]	70 - 75[36]

1. $r_y = \frac{1}{4\pi\sqrt{2}} \left(\frac{K_{I_c}}{\sigma_y}\right)^2$

2. $\gamma' = \frac{G_{I_c}}{2}$

3. Obtained with 1 X 2 SEN specimens; thickness: PC - 0.250 inches, A, PS, VCA - 0.125 inches

Table IV. Effect of specimen geometry on fracture toughness

Specimen	K_{Ic} (ksi(in.)$^{1/2}$)	
	Polycarbonate (1)	Acrylic (2)
1×2 SEN	3.29	0.99
1×4 SEN	3.48	1.41
1×8 SEN	3.68	1.28
1×12 SEN	4.13	1.51
2×4 SEN	3.71	-
3×12 CN	3.81	1.21
1/2 NR	3.97	-
1-1/16 NR	3.79	-

(1) All specimens 0.250 in. thick

(2) All specimens 0.125 in. thick

Table V. Effect of thickness on fracture toughness of polycarbonate

Thickness	K_{Ic} (ksi $(in)^{1/2}$)			
	Sheet	Milled	Laminated (1/8 sheets)	Laminated (1/16 sheets)
0.080	4.00	-	-	-
0.125	3.43	3.67	-	-
0.185	3.25	-	-	-
0.250	3.29	3.57	3.97	4.10
0.375	-	4.05	-	4.45
0.500	-	3.96	-	4.09
0.625	3.73	3.73	-	-

Table VI. Room temperature fracture surface energies ($ergs/cm^2 \times 10^{-5}$)

Method	Acrylic	Polystyrene	Reference
Cleavage	4.9	25.5	29
Cleavage	4.5	9	30
Cleavage	1.4	7.13	31
Tension	2.1	17	32
Fracture mechanics	-	5.5	6
Cleavage	1.25	4.0	37
Fracture mechanics	2.15	4.43	This work

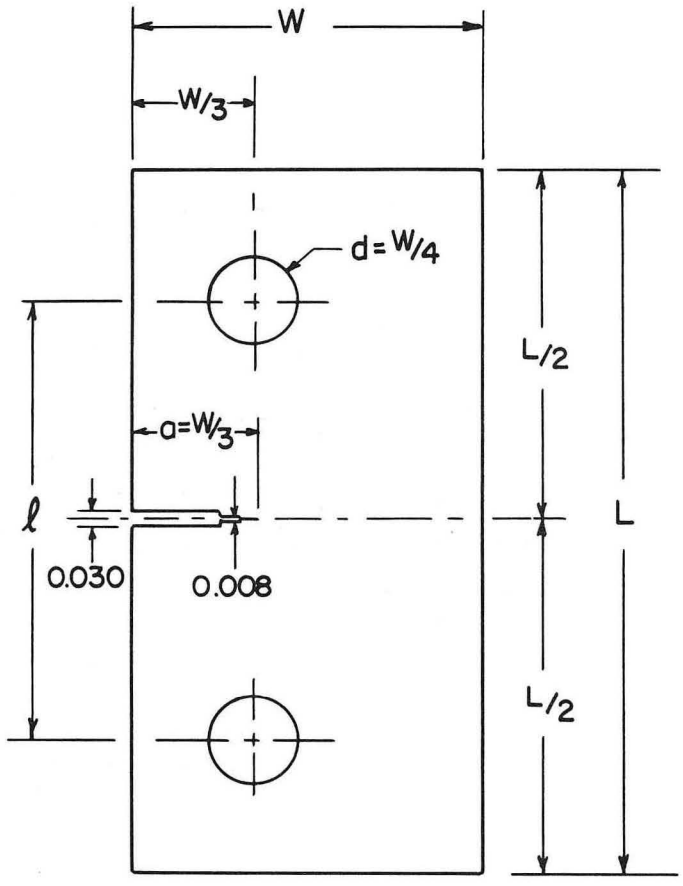

(a)

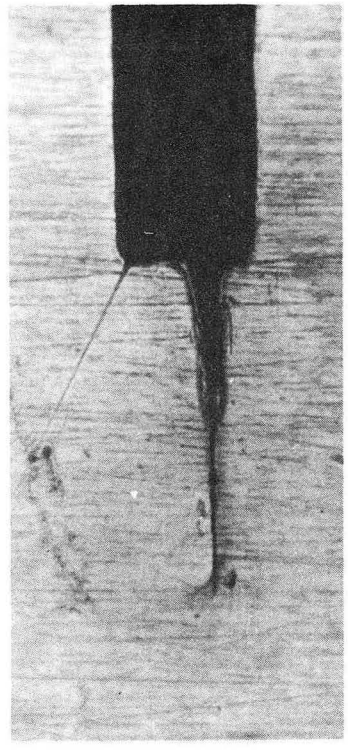

(b)

Specimen	W	L	ℓ	t
SEN 1x2	1	2	1.230	0.080 – 0.625
SEN 2x4	2	4	2.460	0.250
SEN 1x4	1	4	3.230	0.125 or 0.250
SEN 1x8	1	8	7.230	0.125 or 0.250
SEN 1x12	1	12	11.230	0.125 or 0.250

Crack sharpened by razor blade.
Notch radius less than 0.0005 in.

Fig. 1. (a) Dimensions of Single Edge Notched Fracture Specimen.

(b) Typical Crack Tip in Polycarbonate Fracture Specimens. Machined slot 0.008 inch wide extended with a razor blade. 93×

XBB 6711-6540

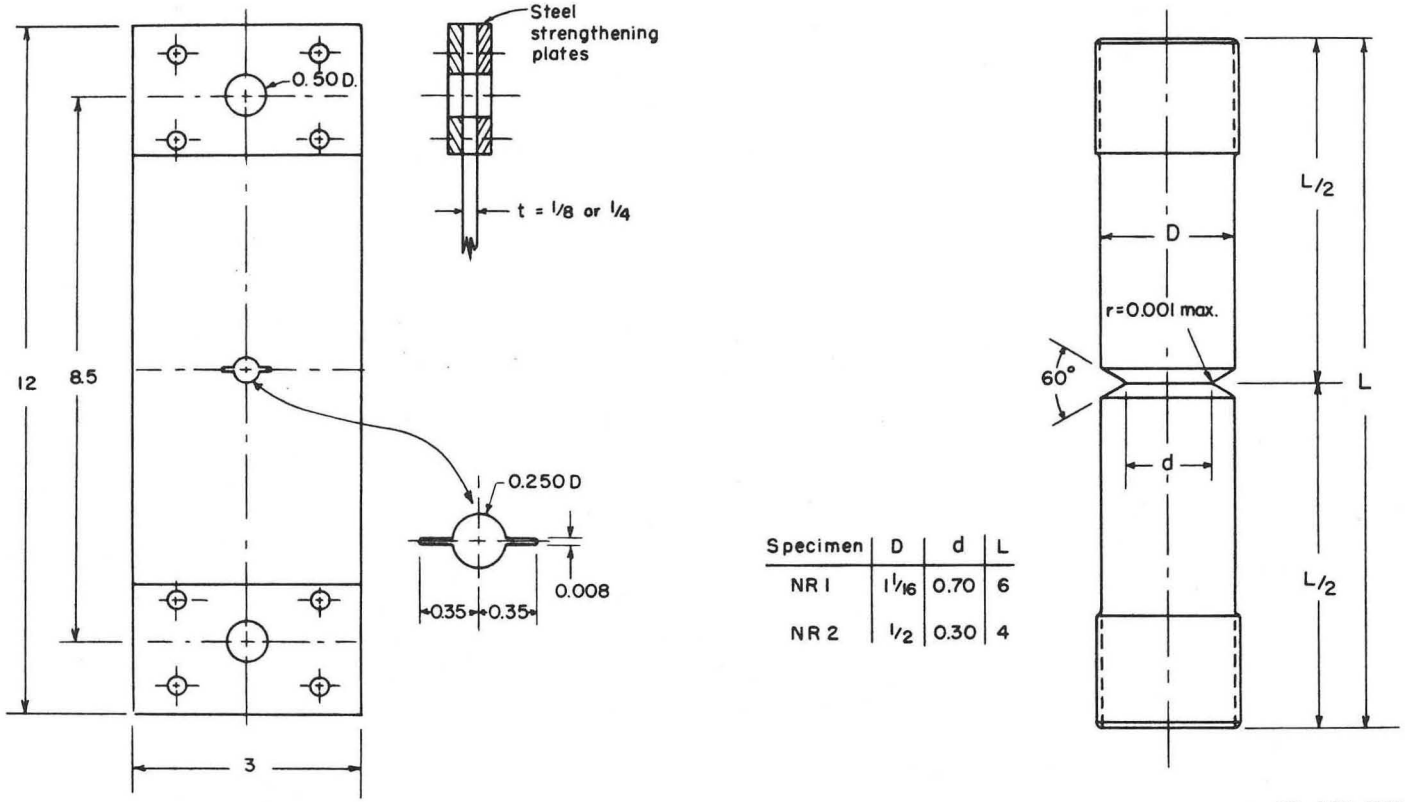

Specimen	D	d	L
NR 1	1 1/16	0.70	6
NR 2	1/2	0.30	4

(a) (b)

Fig. 2 Dimensions of Center Notched (2a) and Notched Round (2b) Fracture Specimens.

(a) Elevated temperature

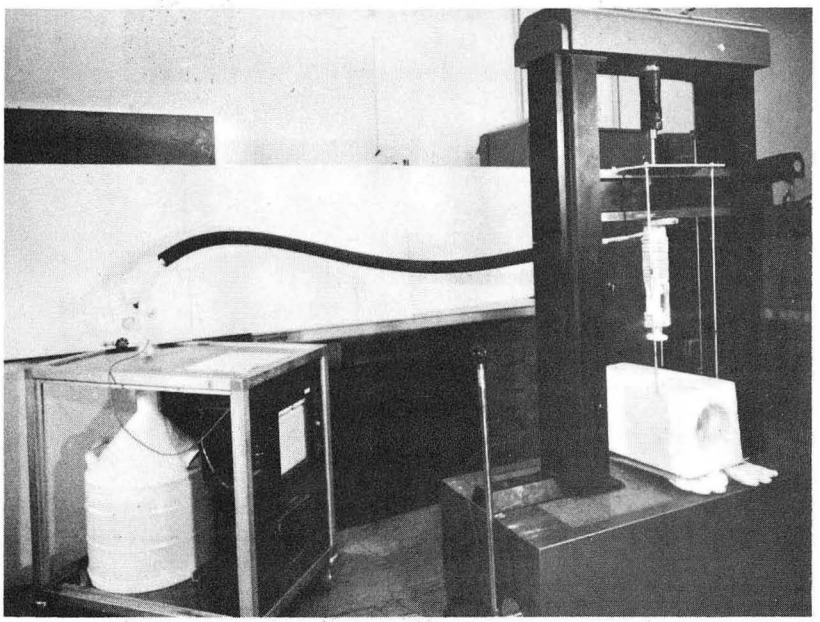

XBB 6711-6589

(b) Low temperature

Fig. 3 Experimental apparatus for low temperature and elevated temperature fracture testing.

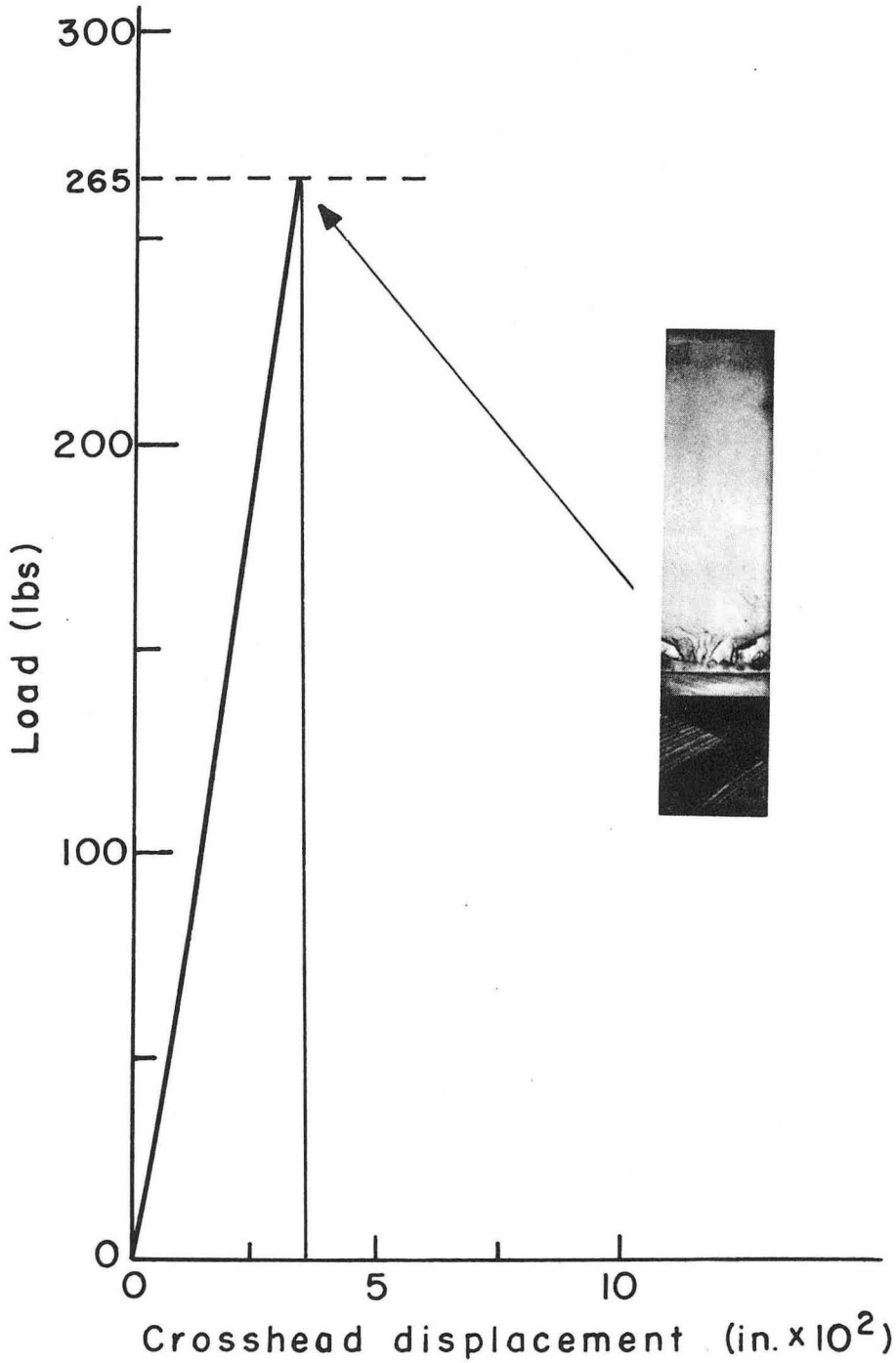

Fig. 4 Load-displacement record for catastrophic fracture with a polycarbonate SEN specimen. Insert shows fracture surface after separation. Test conditions: room temperature and 0.2 cm/min.

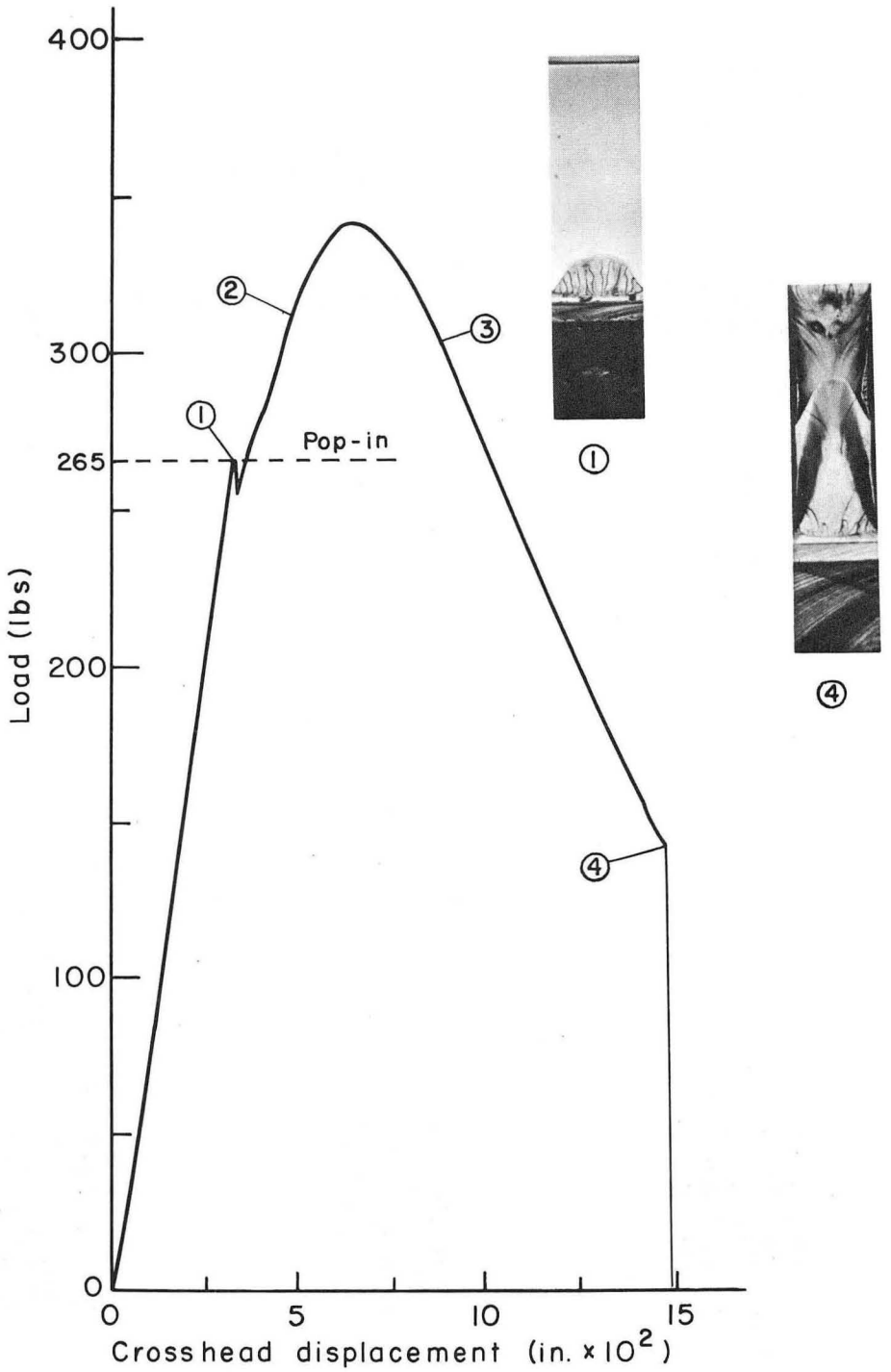

Fig. 5 Load-displacement record for pop-in fracture with a polycarbonate SEN specimen. The plane of fracture just after pop-in as viewed through the specimen is shown in insert 1, the fracture surface after separation is shown in insert 4. Test conditions: room temperature and 0.2 cm/min. Numerals 2 and 3 refer to Fig. 6.

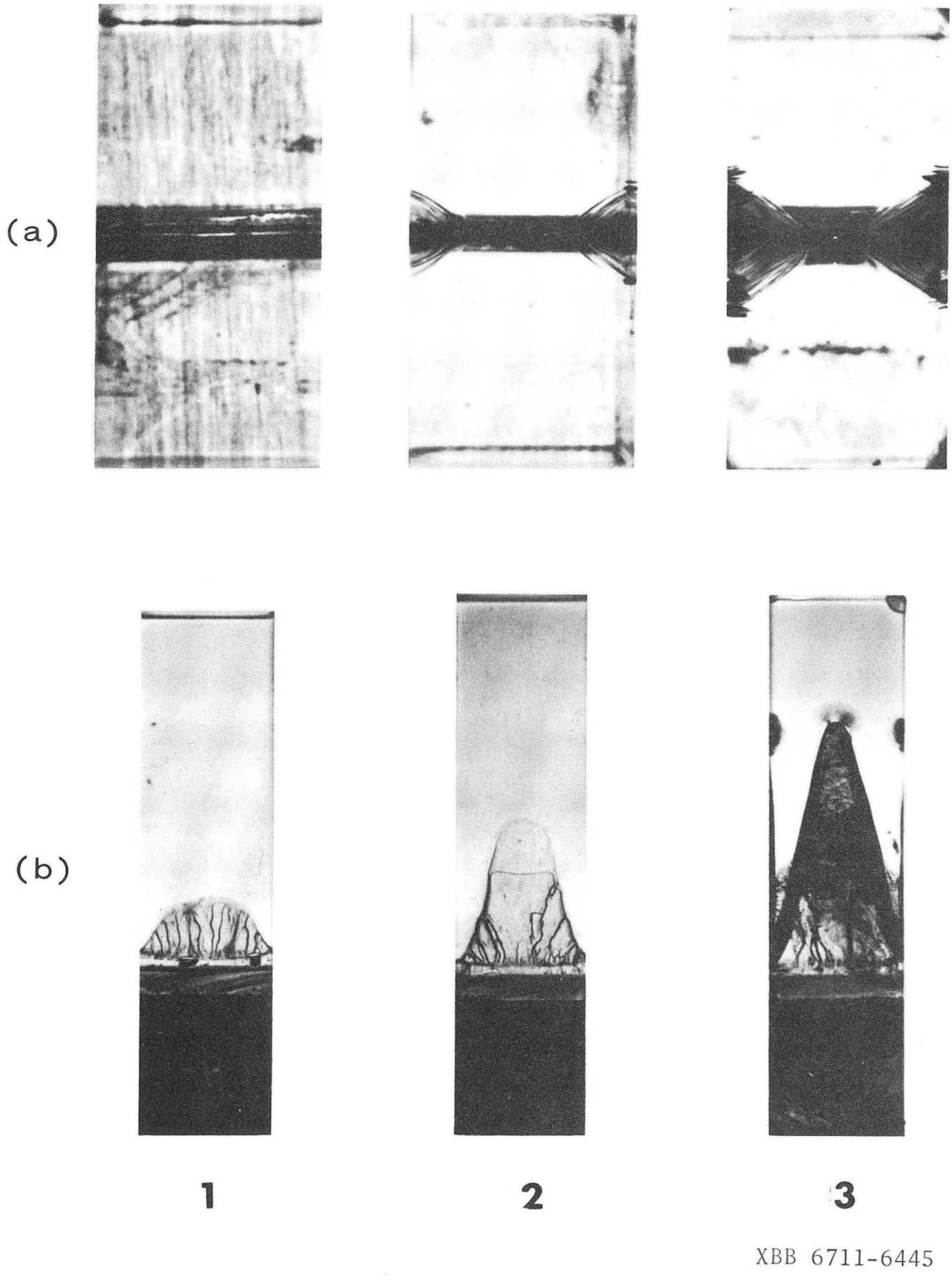

Fig. 6 Development of plastic zones (a) and growth of the central flat region (b) in a pop-in fracture in a SEN polycarbonate specimen. Numbers refer to Fig. 5.

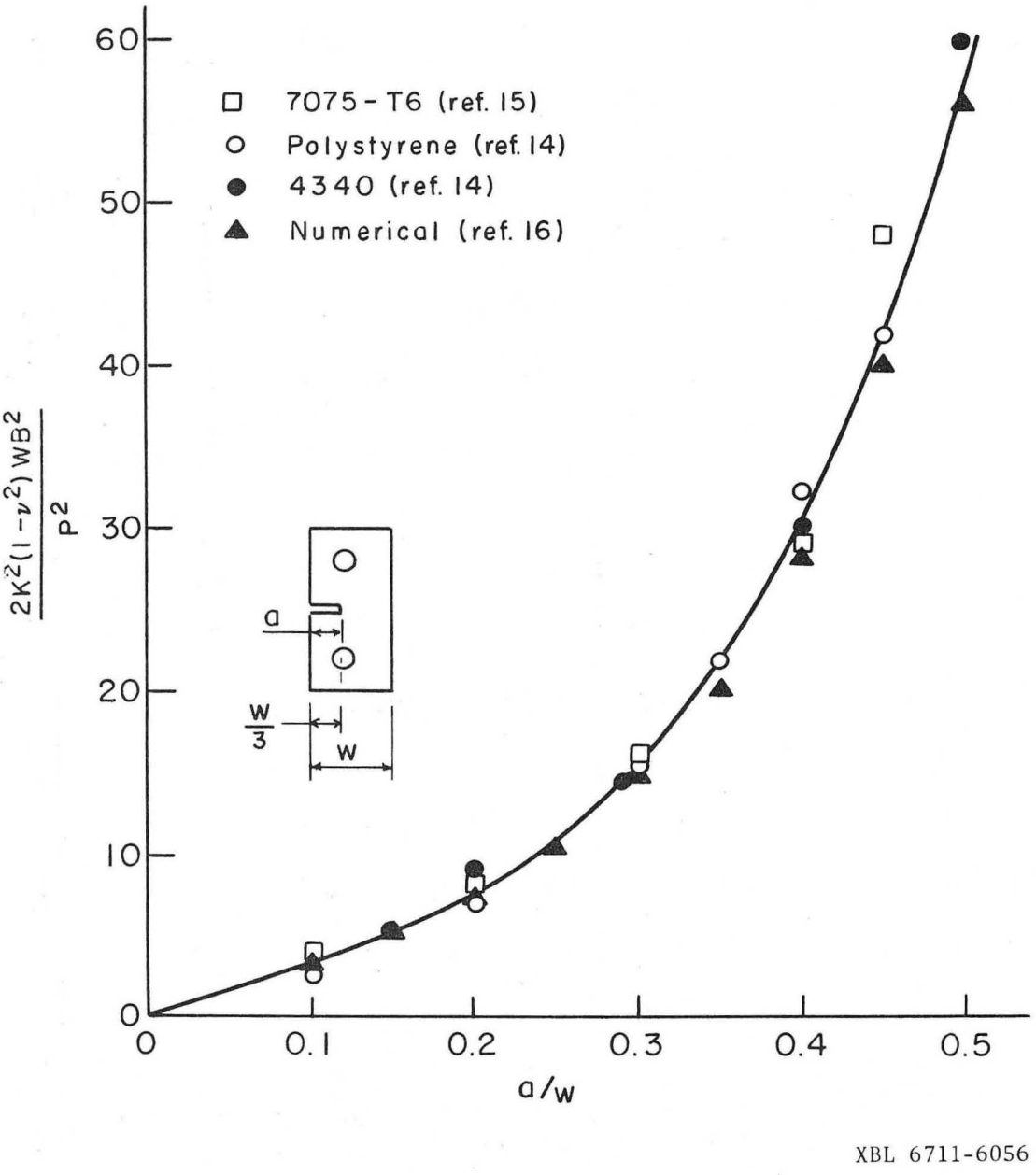

XBL 6711-6056

Fig. 7 Dimensionless Fracture Toughness Parameter for Single Edge Notch Fracture Specimens.

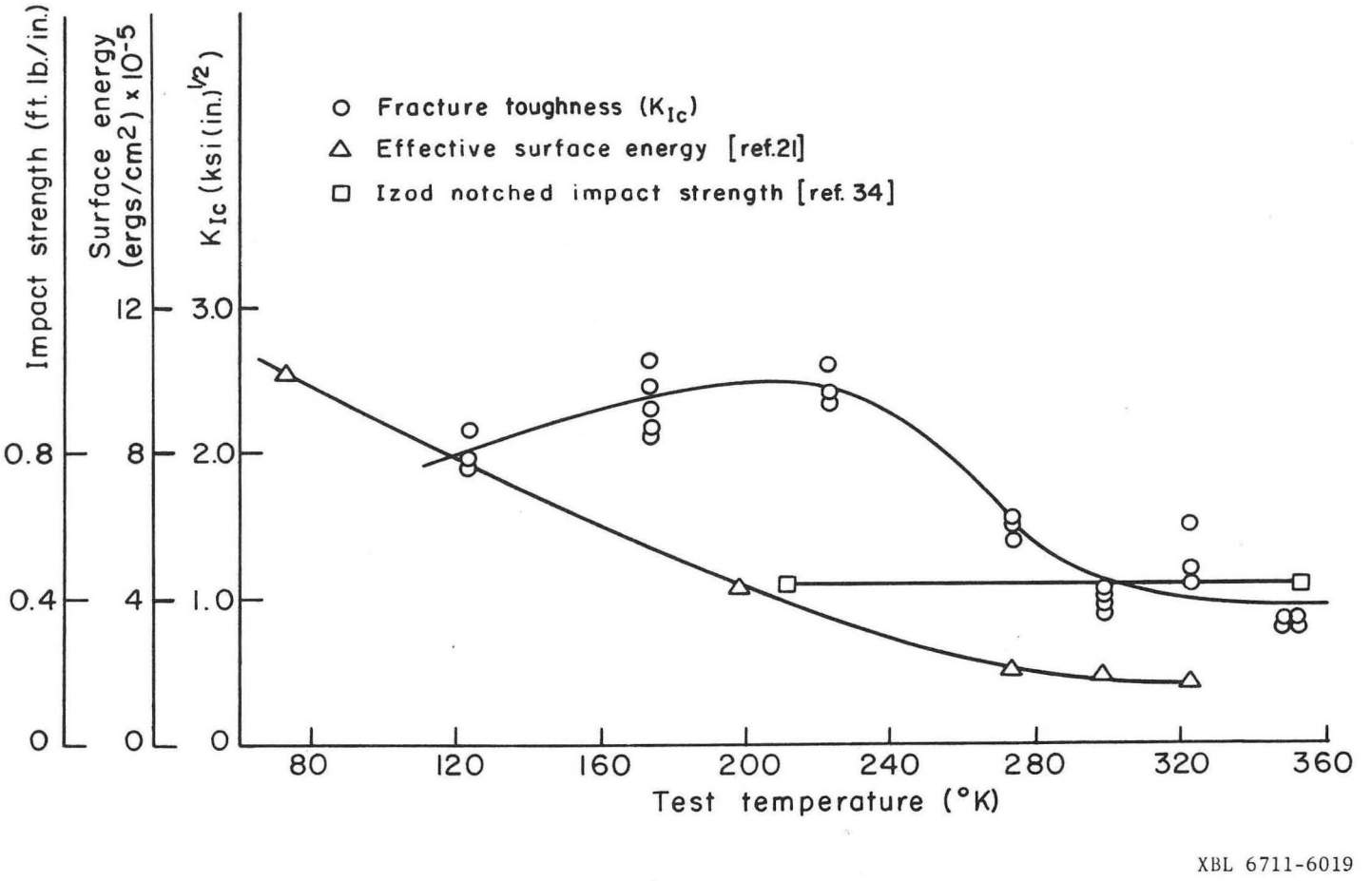

Fig. 8 Effect of Temperature on Fracture Parameters of Acrylic.

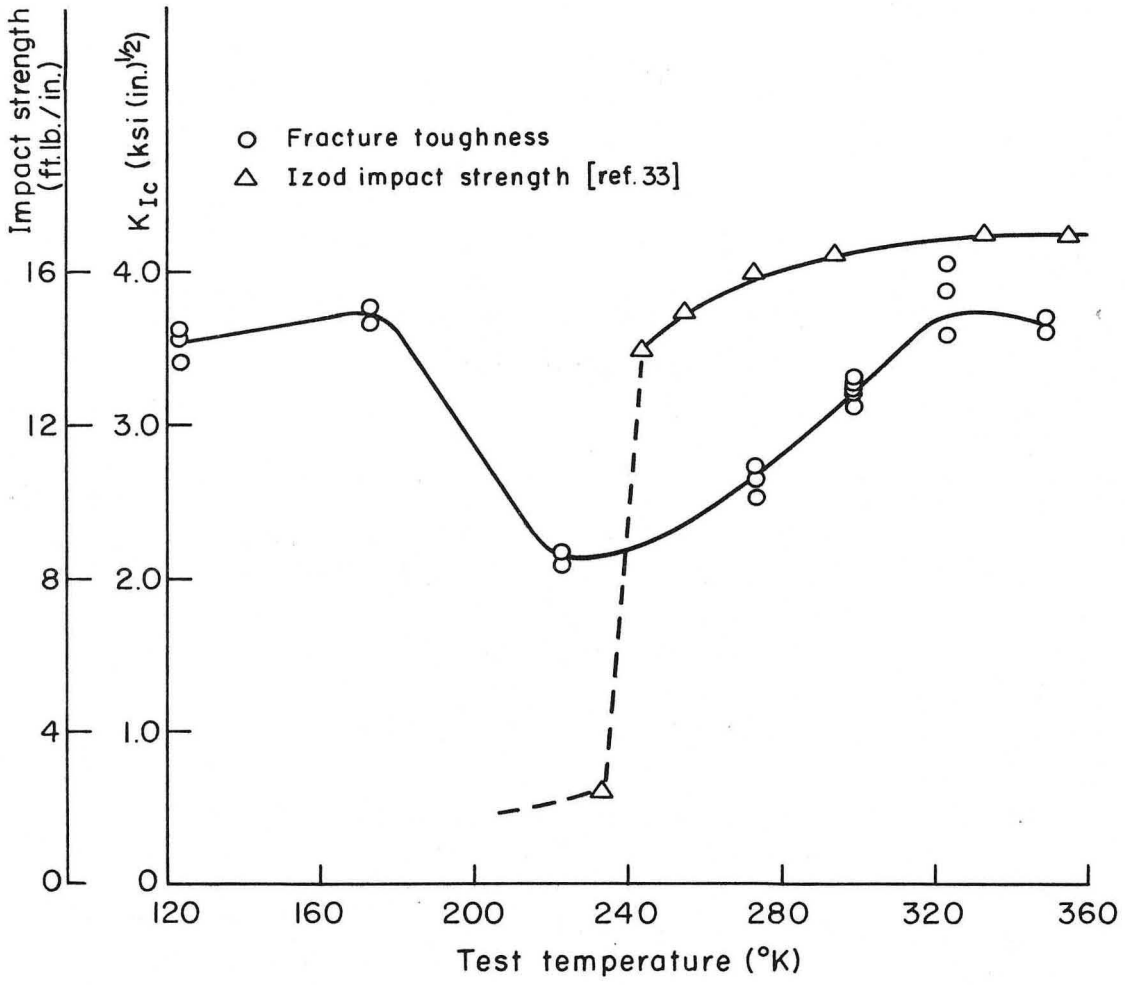

Fig. 9 Effect of Temperature on Fracture Parameters of Polycarbonate.

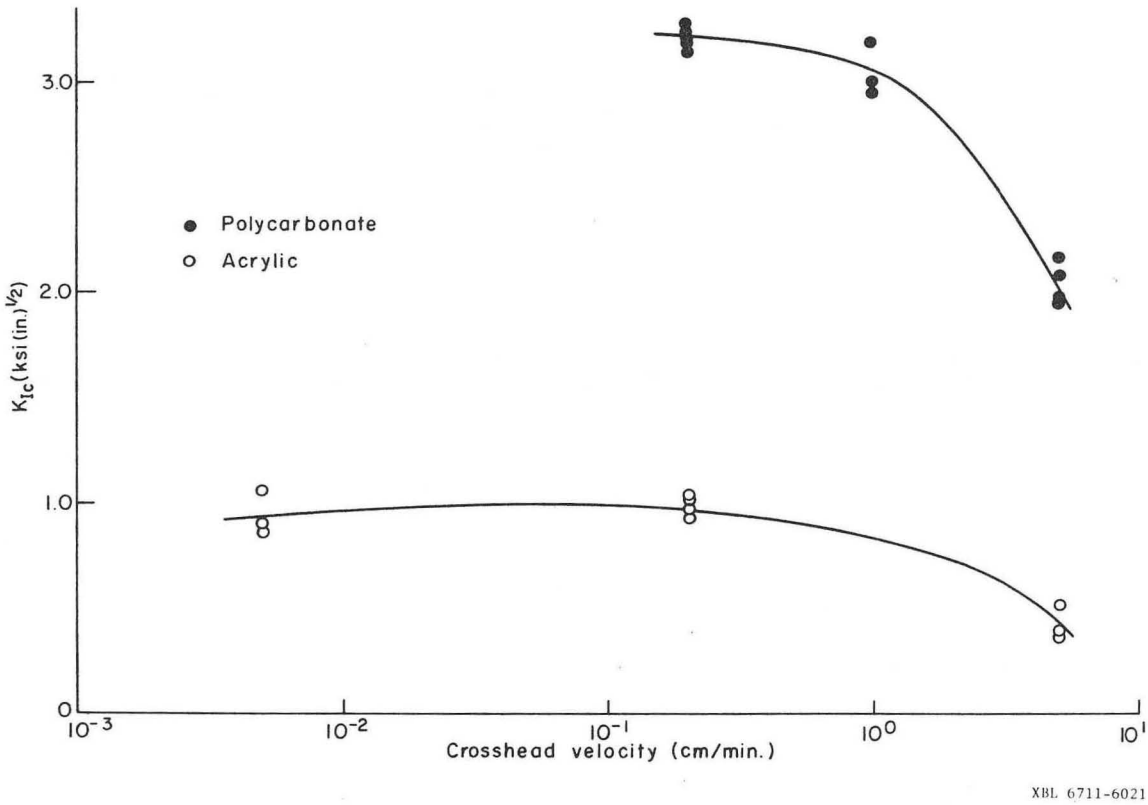

Fig. 10 Effect of Loading Rate on the Room Temperature Fracture Toughness of Acrylic and Polycarbonate.

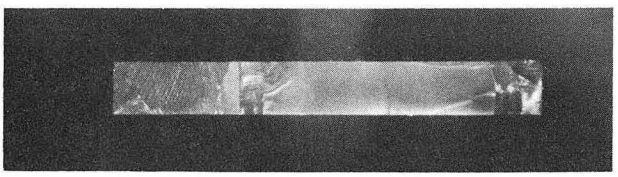

(a) Macroview, 2.2×

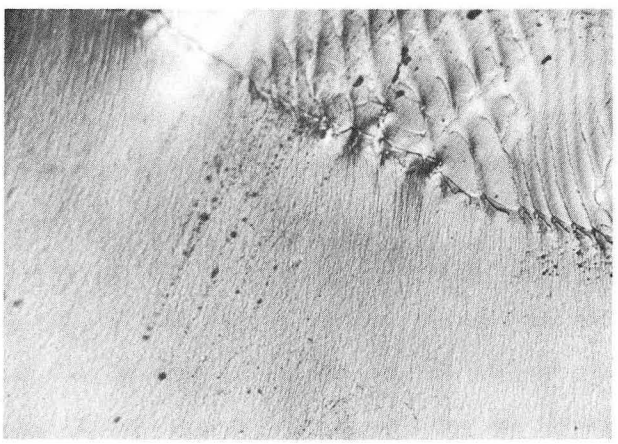

(b) Mirror area adjacent to machined notch, 47.5×

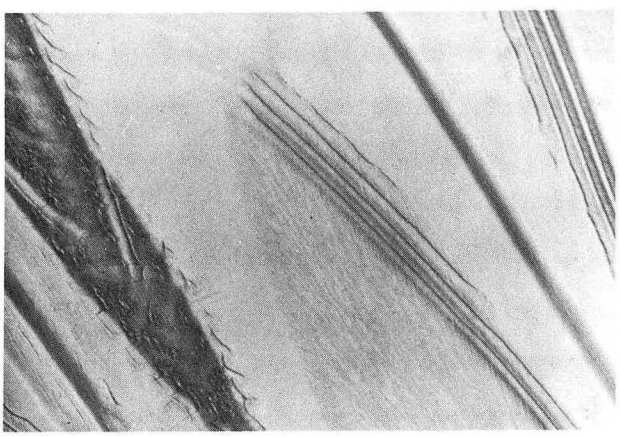

XBB 6711-6542

(c) Fast crack area near middle of fracture surface, 47.5×

Fig. 11 Fracture surface of acrylic SEN specimen. Test conditions: room temperature (300°K) and 0.2 cm/min.

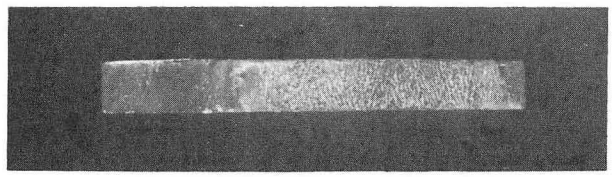

(a) Macroview. 2.2×

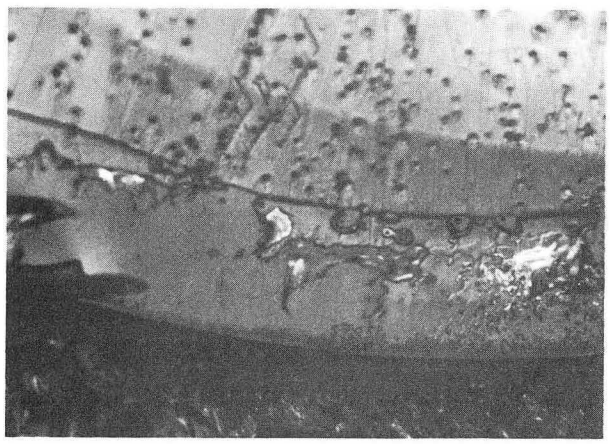

(b) Mirror area adjacent to machined notch. 47.5×

XBB 6711-6438

(c) Fast crack area near middle of fracture surface. 47.5×

Fig. 12 Fracture surface of polystyrene SEN specimen. Test conditions: room temperature (300°K) and 0.2 cm/min.

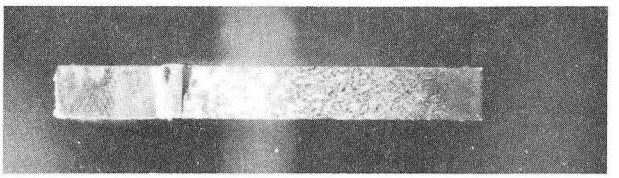

(a) Macroview. 2.2×

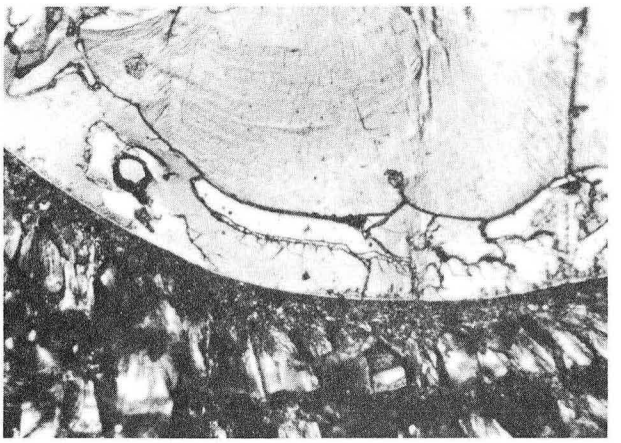

(b) Mirror area adjacent to machined notch. 47.5×

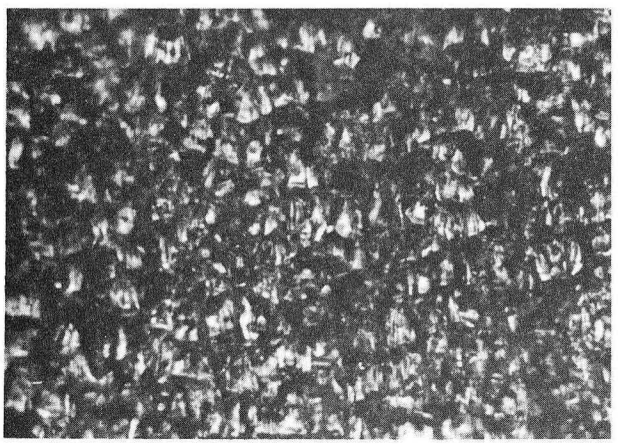

XBB 6711-6460

(c) Fast crack area near middle of fracture surface. 47.5×

Fig. 13 Fracture surface of vinyl chloride-vinyl acetate SEN specimen. Test conditions: room temperature (300°K) 0.2 cm/min.

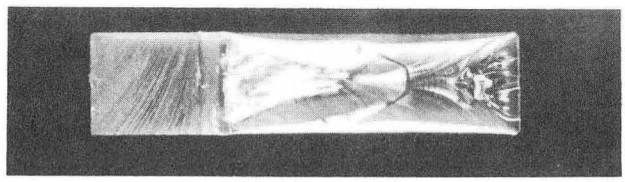

(a) Macroview. 2.2×

(b) Mirror area adjacent to machined notch. 47.5×

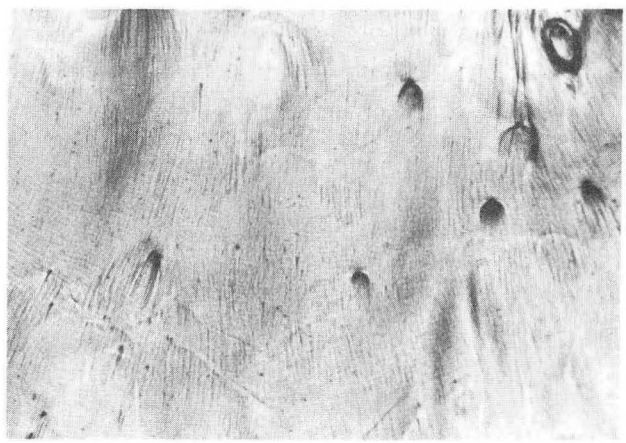

XBB 6711-6459

(c) Fast crack area near middle of fracture surface. 47.5×

Fig. 14 Fracture surface of polycarbonate SEN specimen exhibiting pop-in fracture. Test conditions: room temperature (300°K) and 0.2 cm/min.

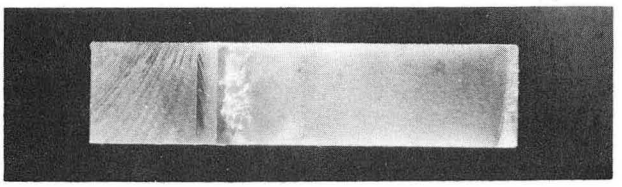

(a) Macroview, 2.2×

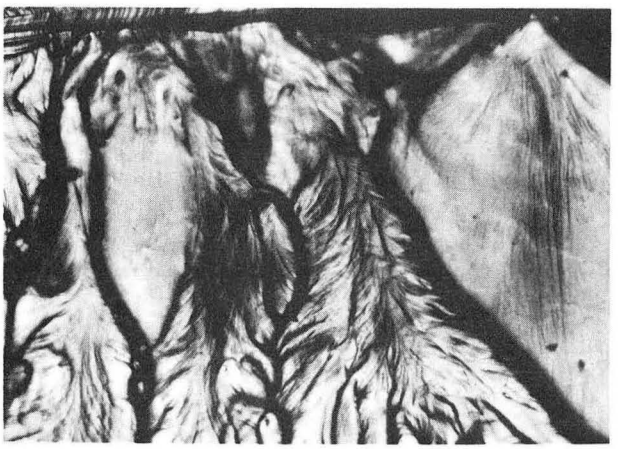

(b) Mirror area adjacent to machined notch, 47.5×

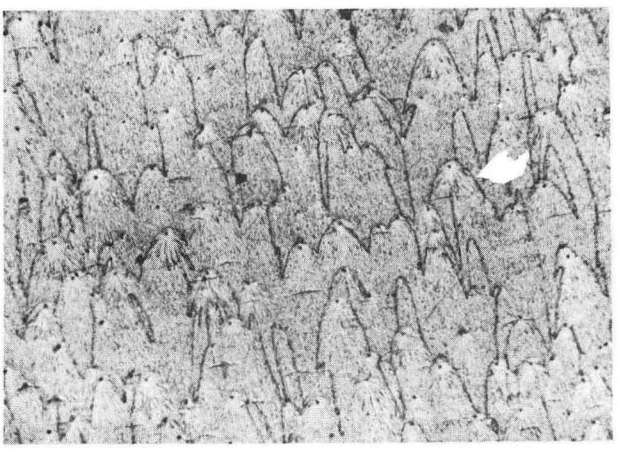

XBB 6711-6541

(c) Fast crack area near middle of fracture surface, 47.5×

Fig. 15 Fracture surface of polycarbonate SEN specimen exhibiting flat fracture. Test conditions: room temperature (300°K) and 0.2 cm/min.

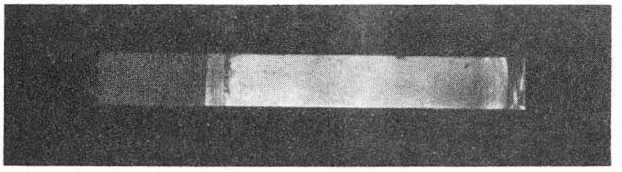

(a) Macroview. 2.2×

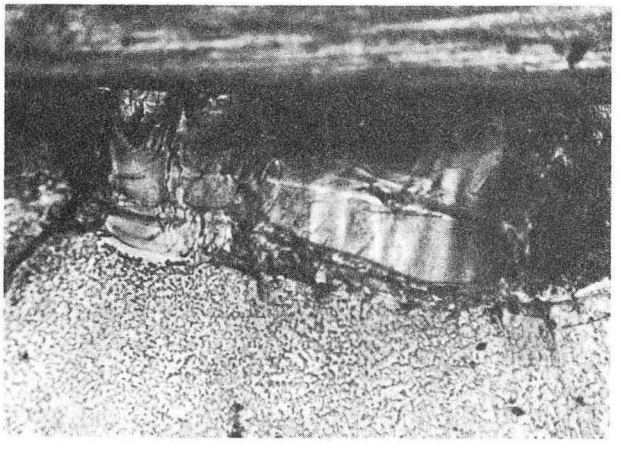

(b) Mirror area adjacent to machined notch. 47.5×

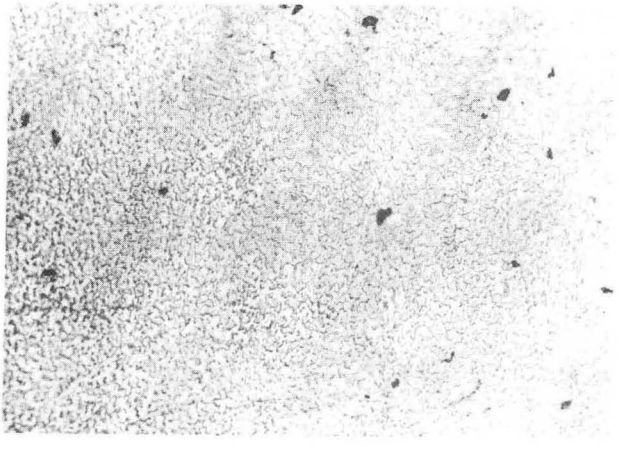

XBB 6711-6451

(c) Fast crack area near middle of fracture surface, 47.5×

Fig. 16 Fracture surface of acrylic SEN specimen tested at 123°K and 0.2 cm/min.

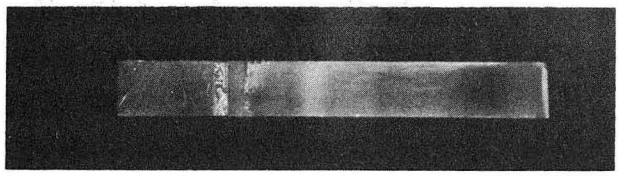

(a) Macroview. 2.2×

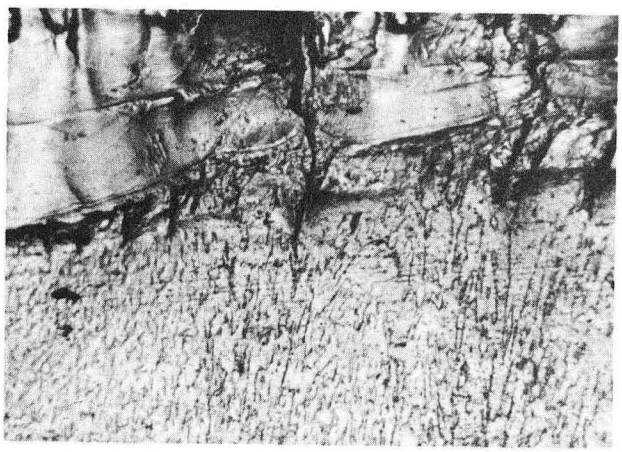

(b) Mirror area adjacent to machined notch. 47.5×

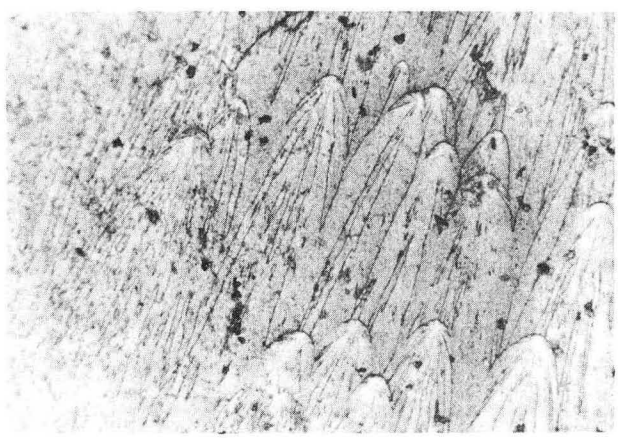

XBB 6711-6452

(c) Fast crack area near middle of fracture surface. 47.5×

Fig. 17 Fracture surface of acrylic SEN specimen tested at 173°K and 0.2 cm/min.

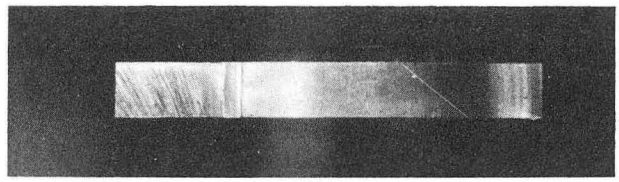

(a) Macroview. 2.2×

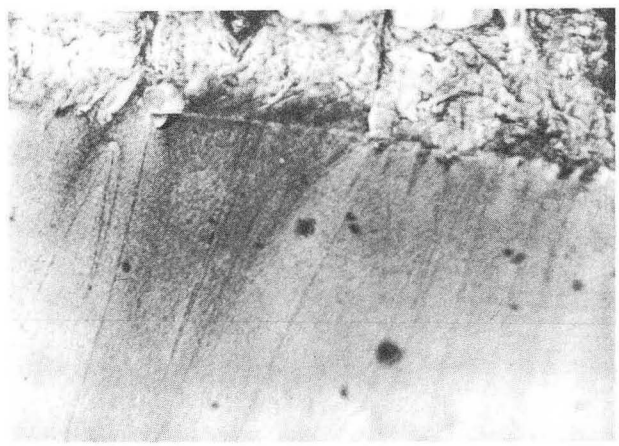

(b) Mirror area adjacent to machined notch. 47.5×

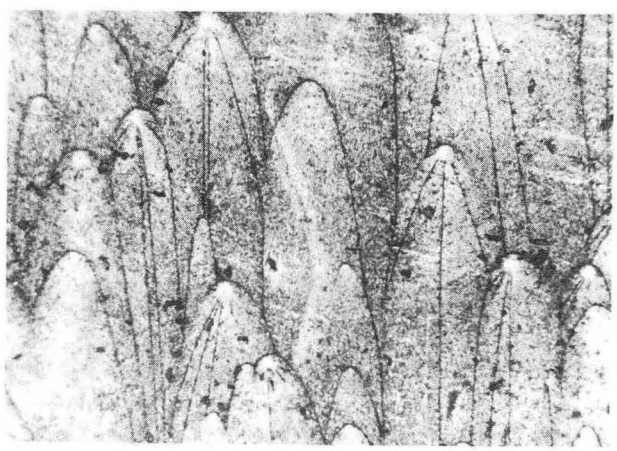

XBB 6711-6453

(c) Fast crack area near middle of fracture surface. 47.5×

Fig. 18 Fracture surface of acrylic SEN specimen tested at 223°K and 0.2 cm/min.

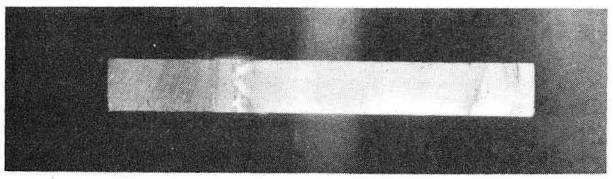

(a) Macroview. 2.2×

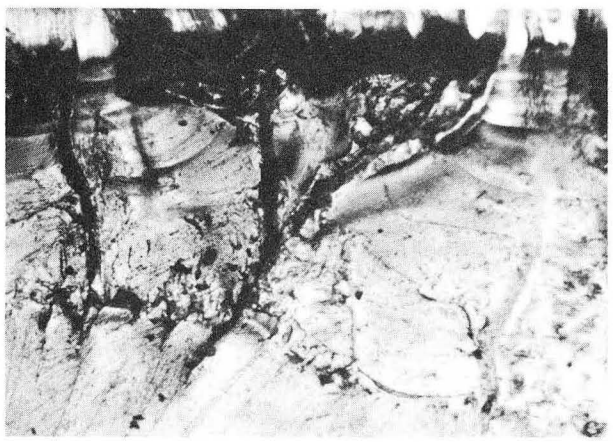

(b) Mirror area adjacent to machined notch. 47.5×

XBB 6711-6454

(c) Fast crack area near middle of fracture surface. 47.5×

Fig. 19 Fracture surface of acrylic SEN specimen tested at 273°K and 0.2 cm/min.

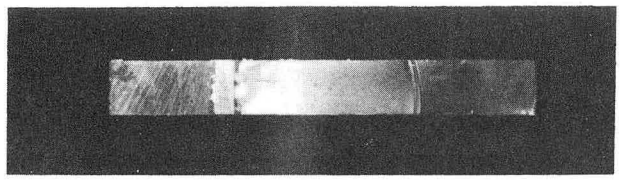

(a) Macroview. 2.2×

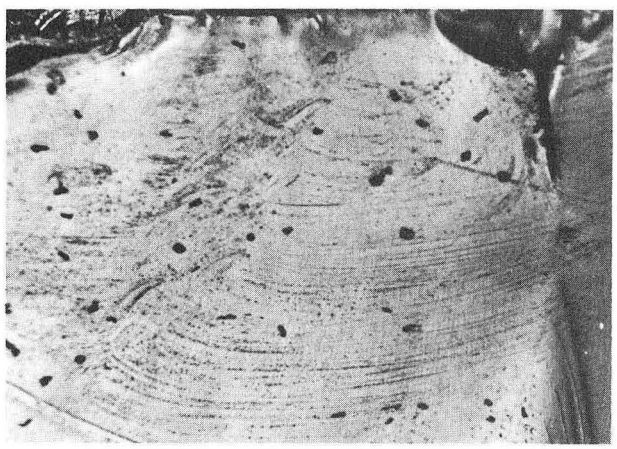

(b) Mirror area adjacent to machined notch. 47.5×

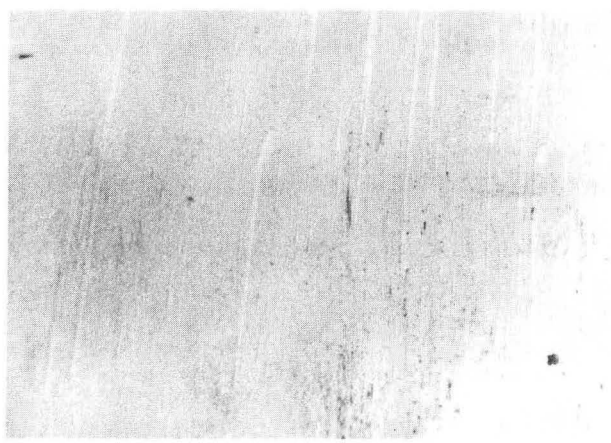

XBB 6711-6455

(c) Fast crack area near middle of fracture surface. 47.5×

Fig. 20. Fracture surface or acrylic SEN specimen tested at 323°K and 0.2 cm/min.

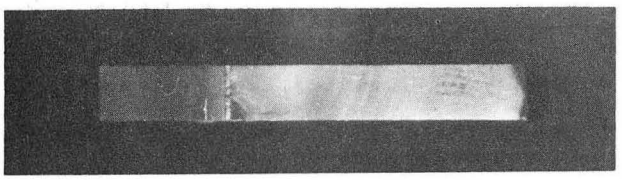

(a) Macroview. 2.2×

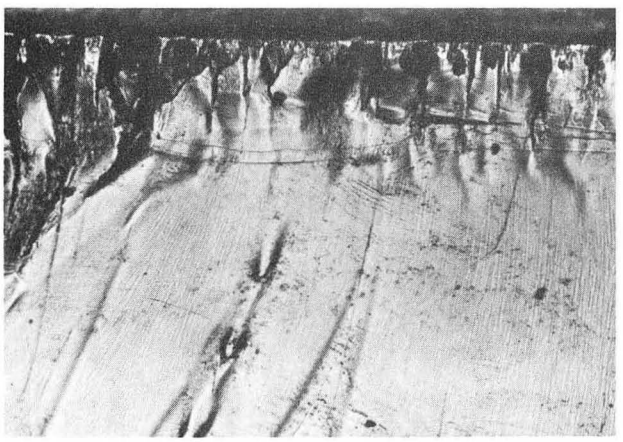

(b) Mirror area adjacent to machined notch. 47.5×

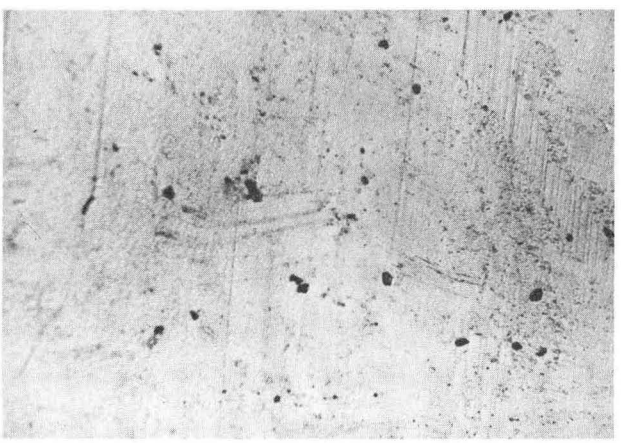

XBB 6711-6444

(c) Fast crack area near middle of fracture surface. 47.5×

Fig. 21 Fracture surface of acrylic SEN specimen tested at 348°K and 0.2 cm/min.

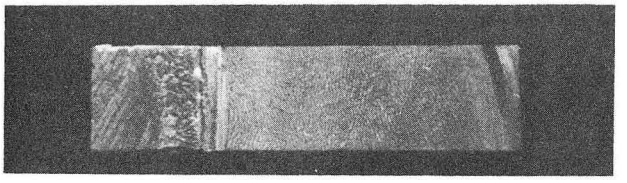

(a) Macroview. 2.2×

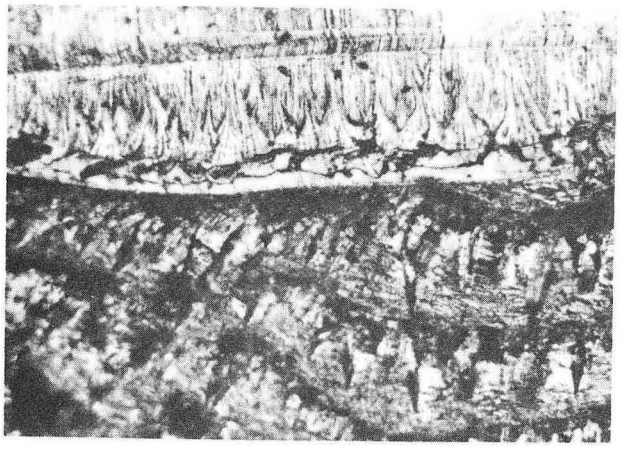

(b) Mirror area adjacent to machined notch. 47.5×

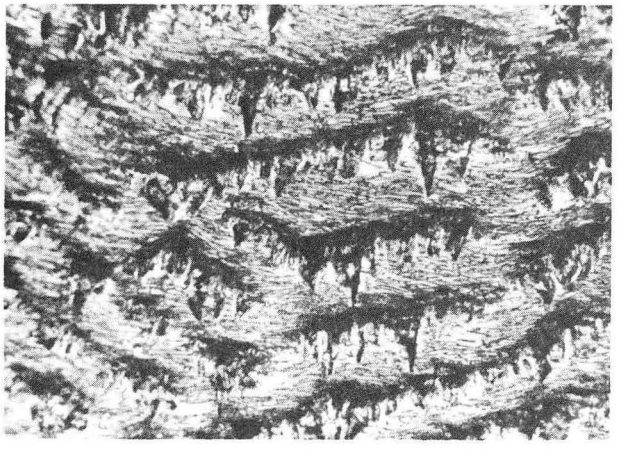

XBB 6711-6657

(c) Fast crack area near middle of fracture surface. 47.5×

Fig. 22 Fracture surface of polycarbonate SEN specimen tested at 123°K and 0.2 cm/min.

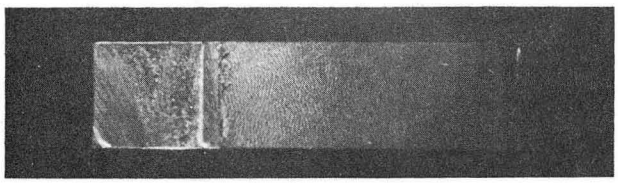

(a) Macroview. 2.2×

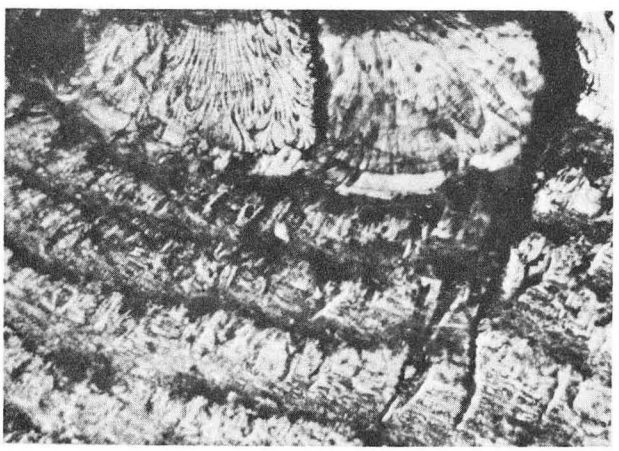

(b) Mirror area adjacent to machined notch. 47.5×

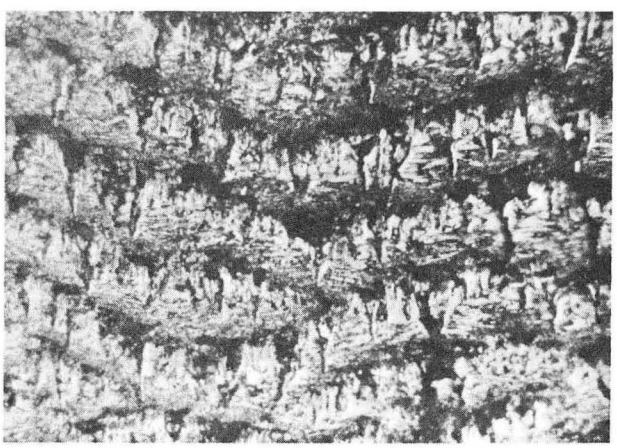

XBB 6711-6658

(c) Fast crack area near middle of fracture surface. 47.5×

Fig. 23 Fracture surface of polycarbonate SEN specimen tested at 173°K and 0.2 cm/min.

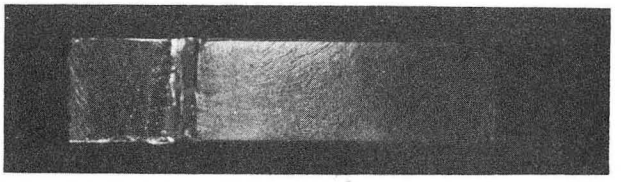

(a) Macroview. 2.2×

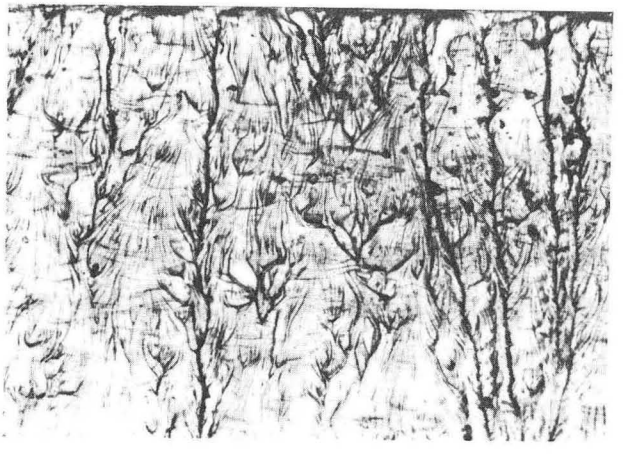

(b) Mirror area adjacent to machined notch. 47.5×

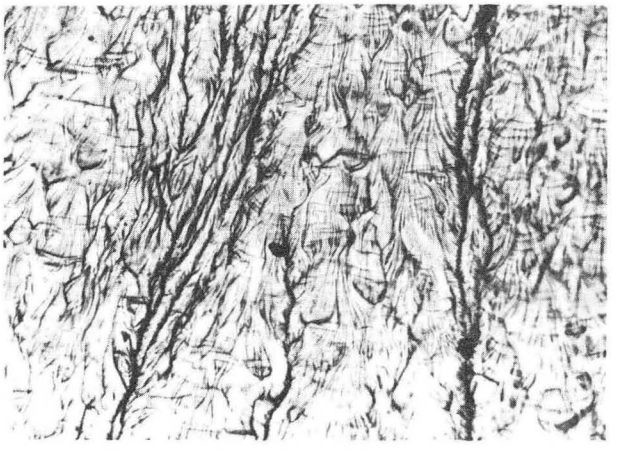

XBB 6711-6441

(c) Fast crack area near middle of fracture surface. 47.5×

Fig. 24 Fracture surface of polycarbonate SEN specimen tested at 223°K and 0.2 cm/min.

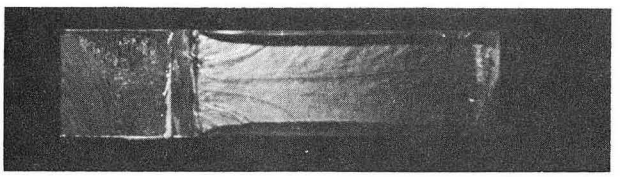

(a) Macroview. 2.2×

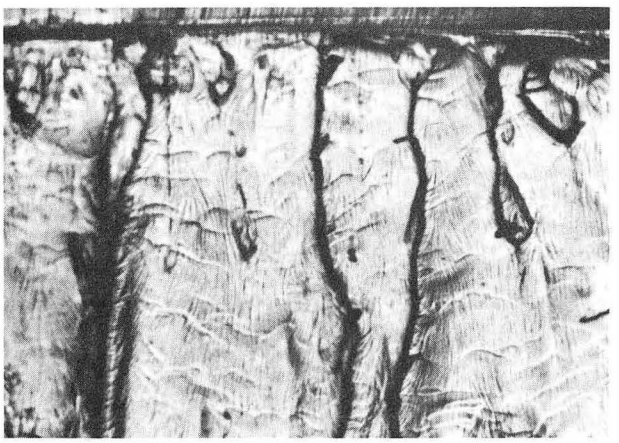

(b) Mirror area adjacent to machined notch. 47.5×

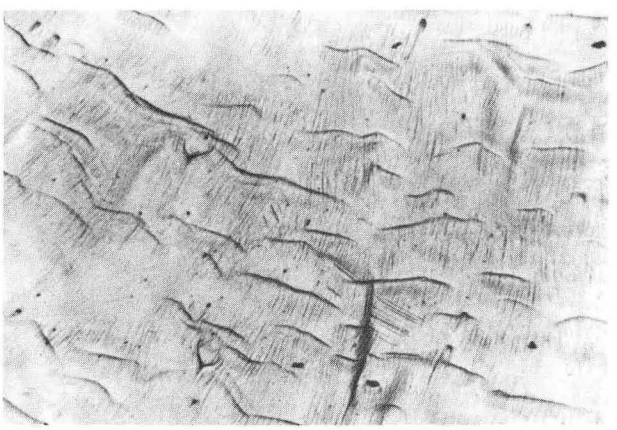

XBB 6711-6442

(c) Fast crack area near middle of fracture surface. 47.5×

Fig. 25 Fracture surface of polycarbonate SEN specimen tested at 273°K and 0.2 cm/min.

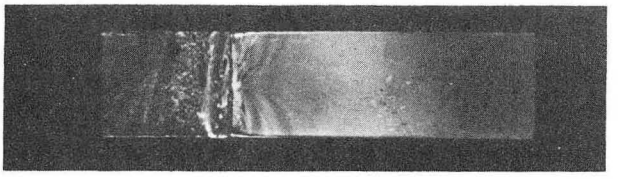

(a) Macroview. 2.2×

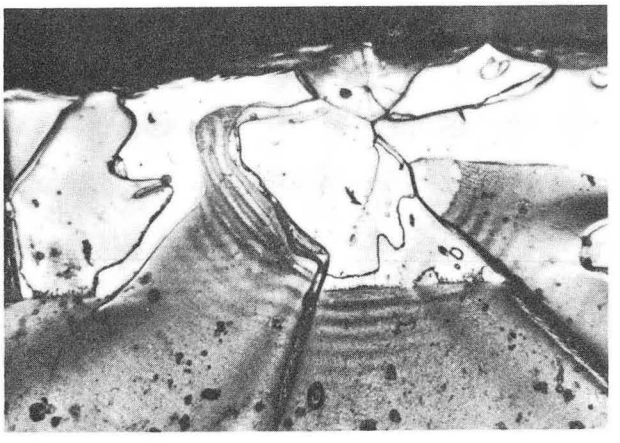

(b) Mirror area adjacent to machined notch. 47.5×

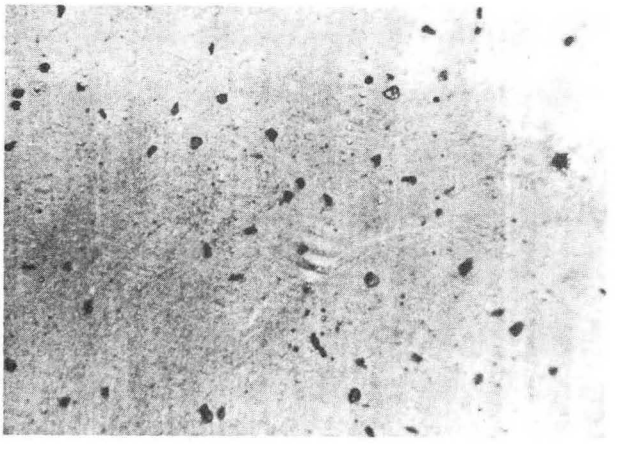

XBB 6711-6440

(c) Fast crack area near middle of fracture surface. 47.5×

Fig. 26 Fracture surface of polycarbonate SEN specimen tested at 323°K and 0.2 cm/min.

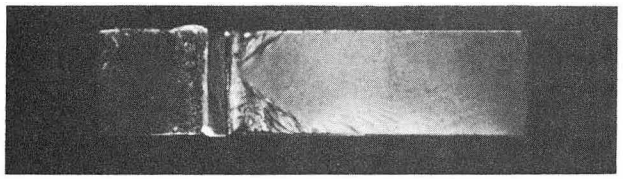

(a) Macroview. 2.2×

(b) Mirror area adjacent to machined notch. 47.5×

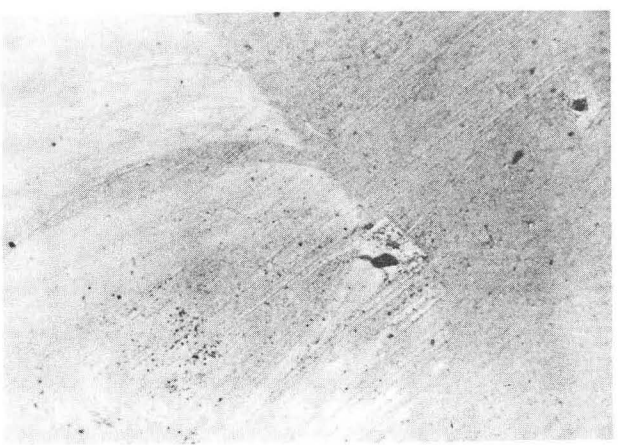

XBB 6711-6439

(c) Fast crack area near middle of fracture surface. 47.5×

Fig. 27 Fracture surface of polycarbonate SEN specimen tested at 348°K and 0.2 cm/min.

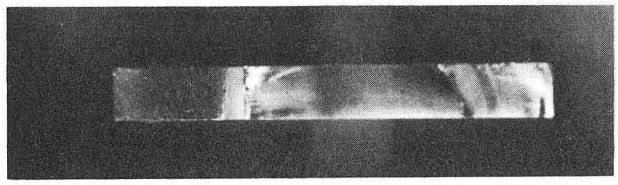

(a) Macroview. 2.2×

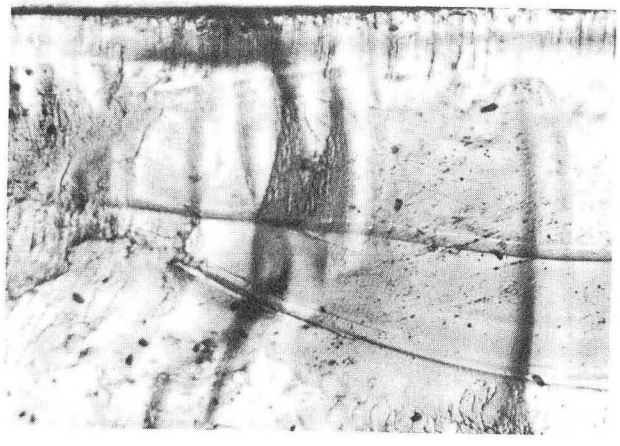

(b) Mirror area adjacent to machined notch. 47.5×

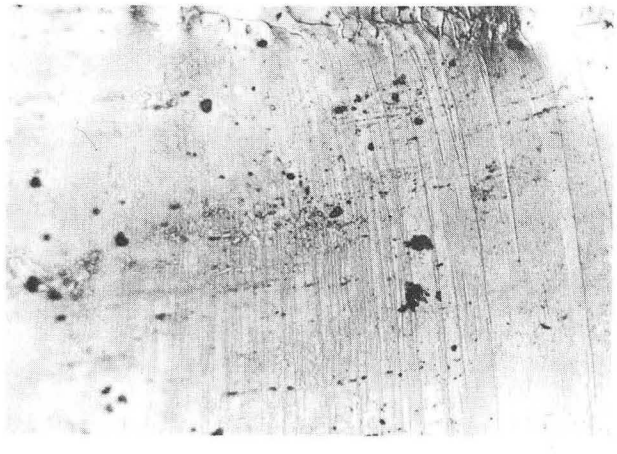

XBB 6711-6449

(c) Fast crack area near middle of fracture surface. 47.5×

Fig. 28 Fracture surface of acrylic SEN specimen tested at 5×10^{-3} cm/min and room temperature (300°K).

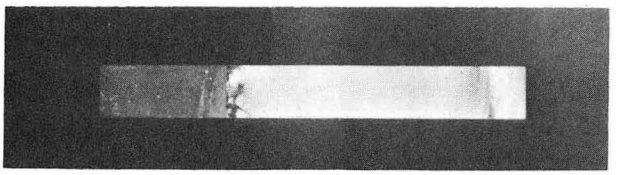

(a) Macroview. 2.2×

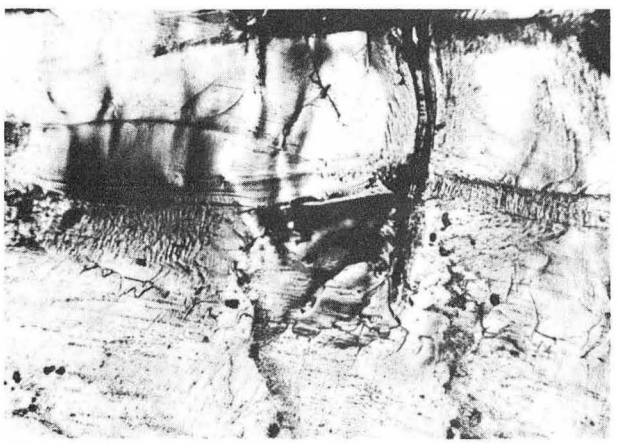

(b) Mirror area adjacent to machined notch. 47.5×

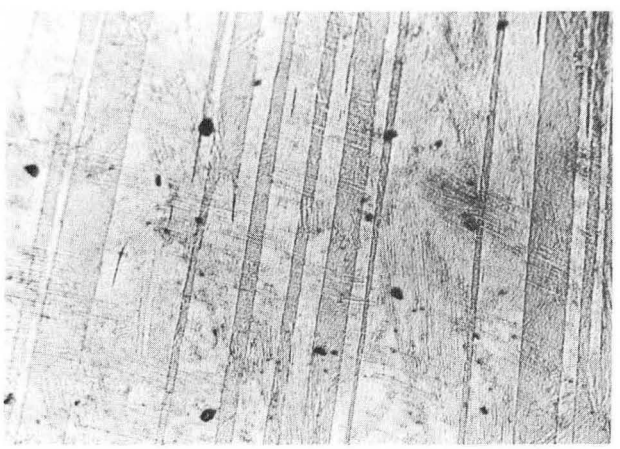

XBB 6711-6450

(c) Fast crack area near middle of fracture surface. 47.5×

Fig. 29 Fracture surface of acrylic SEN specimen tested at 5 cm/min and room temperature (300°K).

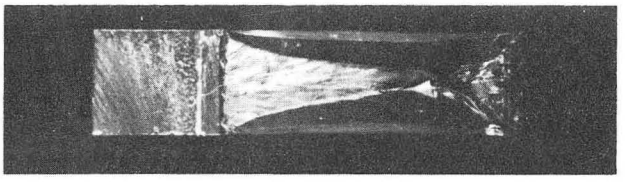

(a) Macroview. 2.2×

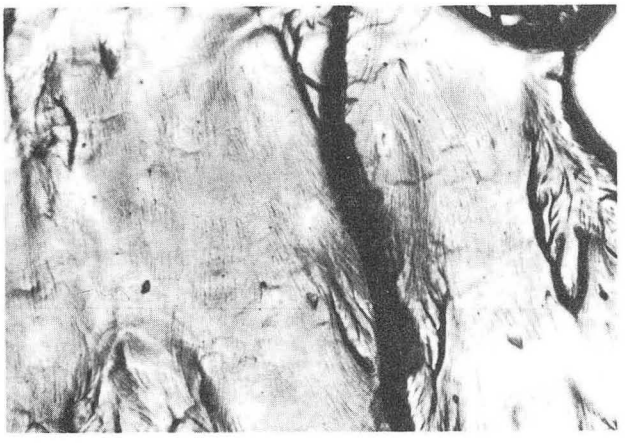

(b) Mirror area adjacent to machined notch. 47.5×

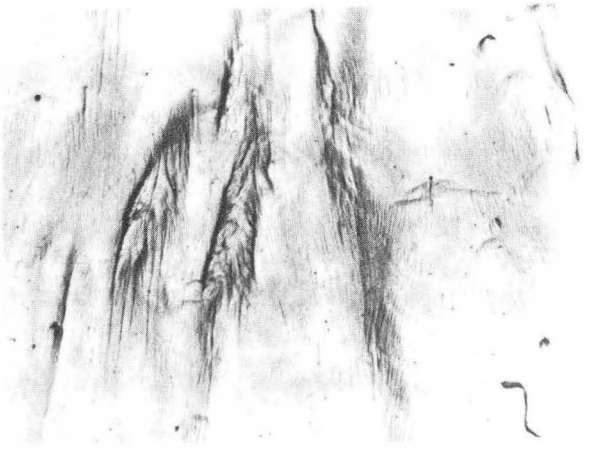

XBB 6711-6456

(c) Fast crack area near middle of fracture surface. 47.5×

Fig. 30 Fracture surface of polycarbonate SEN specimen tested at 1 cm/min and room temperature (300°K).

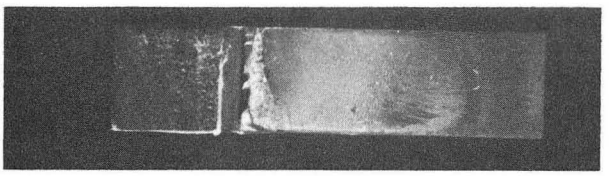

(a) Macroview. 2.2×

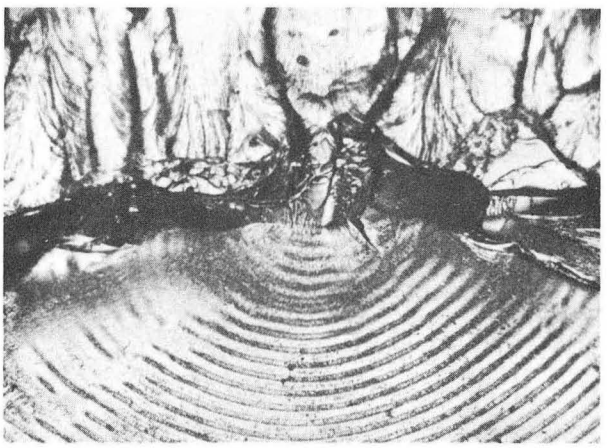

(b) Mirror area adjacent to machined notch 47.5×

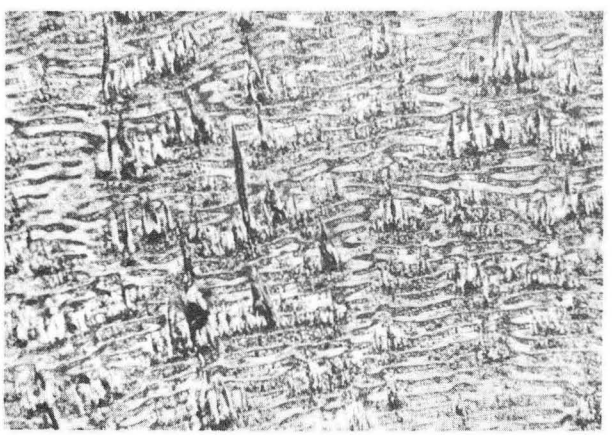

XBB 6711-6443

(c) Fast crack area near middle of fracture surface. 47.5×

Fig. 31 Fracture surface of polycarbonate SEN specimen tested at 5 cm/min and room temperature (300°K).

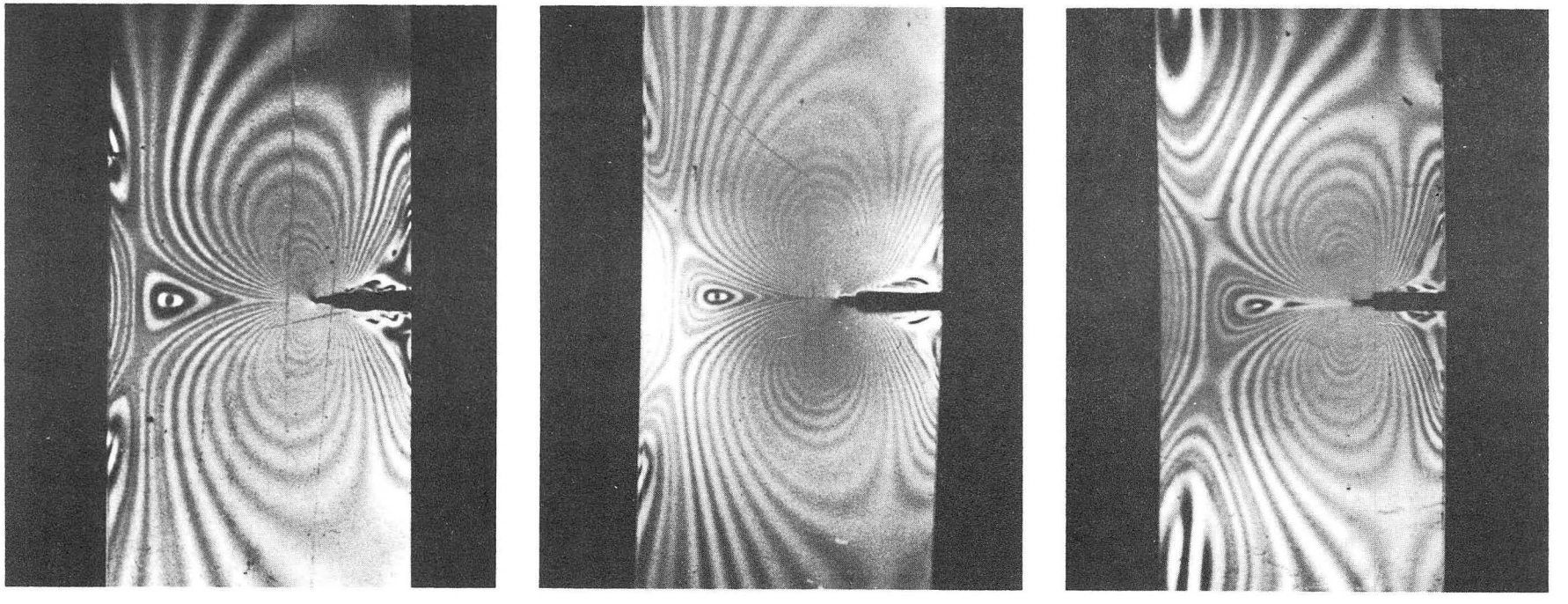

XBB 6711-6457

(a) 1×4 SEN (b) 1×8 SEN (c) 1×12 SEN

Fig. 32 Isochromatic patterns with polycarbonate SEN specimens of various lengths loaded to a stress intensity factor slightly less than critical ($K=3.0$ ksi$(in)^{1/2}$; $K_{Ic}=3.2$ ksi$(in)^{1/2}$. Black and white pattern reproduced from colored pattern obtained with white light and a circular polariscope with quarterwave plates in opposition. Specimen thickness 0.250 inches, material fringe value = 81 psi(in)/fringe. 1.8×

UCRL-17911

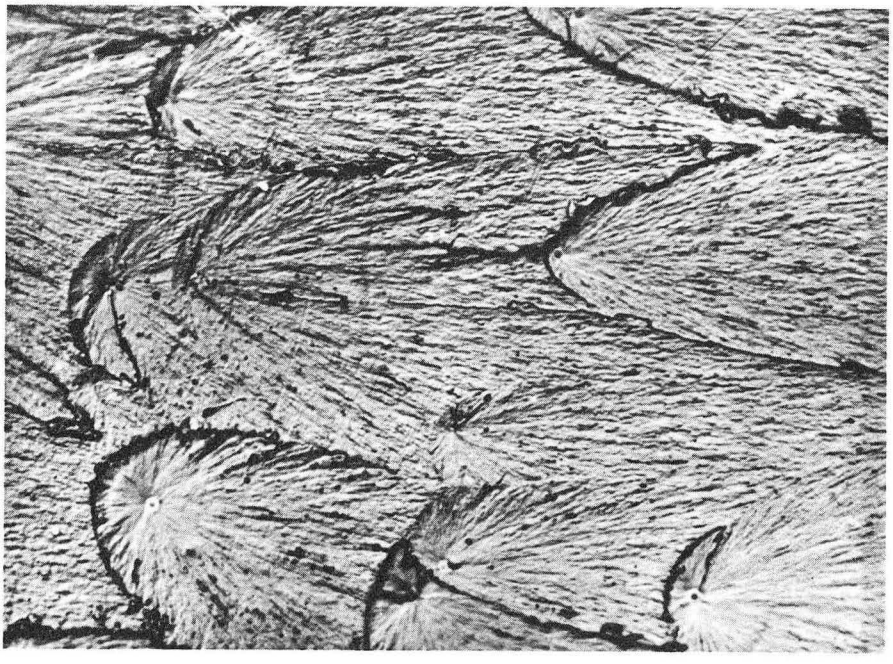

XBB 6711-6458

Fig. 33 Parabola markings on polycarbonate fracture surface. Test conditions: room temperature (300°K) and 0.2 cm/min. 710×